Journal Pre-proofs

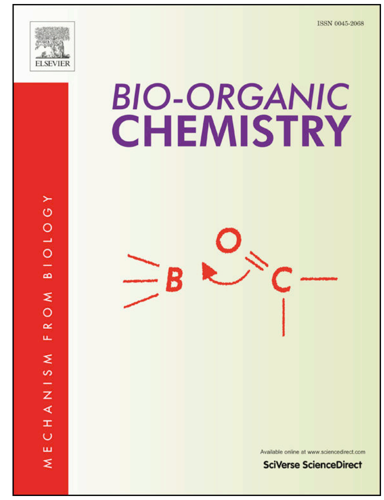

Design and Synthesis of some new 2,4,6-trisubstituted quinazoline EGFR inhibitors as targeted anticancer agents

Heba Abdelrasheed Allam, Enayat E. Aly, Ahmed K.B.A.W. Farouk, Ahmed M. El Kerdawy, Essam Rashwan, Safinaz E.S. Abbass

PII: S0045-2068(20)30106-1
DOI: https://doi.org/10.1016/j.bioorg.2020.103726
Reference: YBIOO 103726

To appear in: *Bioorganic Chemistry*

Received Date: 14 January 2020
Revised Date: 20 February 2020
Accepted Date: 4 March 2020

Please cite this article as: H. Abdelrasheed Allam, E.E. Aly, A.K.B. Farouk, A.M. El Kerdawy, E. Rashwan, S.E.S. Abbass, Design and Synthesis of some new 2,4,6-trisubstituted quinazoline EGFR inhibitors as targeted anticancer agents, *Bioorganic Chemistry* (2020), doi: https://doi.org/10.1016/j.bioorg.2020.103726

Design and Synthesis of some new 2,4,6-trisubstituted quinazoline EGFR inhibitors as targeted anticancer agents

Heba Abdelrasheed Allam[1], Enayat E. Aly[1], Ahmed K. B. A. W. Farouk[1], Ahmed M. El Kerdawy[1,2], Essam Rashwan[3], Safinaz E. S. Abbass[1]

[1]*Department of Pharmaceutical Chemistry, Faculty of Pharmacy, Cairo University, Kasr El-Aini Street, Cairo, P.O. Box, 11562, Egypt*

[2]*Department of Pharmaceutical Chemistry, Faculty of Pharmacy, New Giza University, Newgiza, km 22 Cairo–Alexandria Desert Road, Cairo, Egypt*

[3]*Head of Confirmatory Diagnostic Unit, VACSERA, Cairo, Egypt*

---

*Corresponding author: Heba Abdelrasheed Allam

E-mail: hebaallam80@hotmail.com ; Tel: +201006377655.

Design and Synthesis of some new 2,4,6-trisubstituted quinazoline EGFR inhibitors as targeted anticancer agents

Heba Abdelrasheed Allam[1], Enayat E. Aly[1], Ahmed K. B. A. W. Farouk[1], Ahmed M. El Kerdawy[1,2], Essam Rashwan[3], Safinaz E. S. Abbass[1]

[1]*Department of Pharmaceutical Chemistry, Faculty of Pharmacy, Cairo University, Kasr El-Aini Street, Cairo, P.O. Box, 11562, Egypt*

[2]*Department of Pharmaceutical Chemistry, Faculty of Pharmacy, New Giza University, Newgiza, km 22 Cairo–Alexandria Desert Road, Cairo, Egypt*

[3]*Confirmatory Diagnostic Unit, VACSERA, Cairo, Egypt*

Abstract

The present study describes the synthesis of 6-bromo-2-(pyridin-3-yl)-4-substituted quinazolines starting from 4-chloro derivative **VI** via the reaction with either phenolic compounds to obtain **VIIa-f**, **IXa-d**, 2-amino-6-(un)substituted benzothiazole to produce **VIIIa-c** or hydrazine hydrate to give **X**. Reaction of the hydrazino functionality of **X** with appropriate acid anhydride, acid chloride or aldehyde affords **XIa-c**, **XIIa-c** and **XIVa-i**, respectively. The target compounds were screened for their efficacy as EGFR inhibitors compared to gefitinib. Compounds eliciting superior EGFR inhibitory activity were further screened for their *in vitro* cytotoxicity against two human cancer cell lines namely: **MCF7** (breast) and **A549** (lung), in addition to normal fibroblast cell **WI38** relative to gefitinib as a reference. Furthermore, compounds that showed potent inhibitory activity on wild-type EGFR were screened against mutant EGFR and assayed for their cytotoxicity against mutant EGFR-expressing cell lines **PC9** and **HCC827**. The unsubstituted benzothiazol-2-amine **VIIa** showing superior EGFR inhibition (IC_{50} = 0.096 μM) and anticancer activity against **MCF-7** cell line (IC_{50} = 2.49 μM) was subjected to cell cycle analysis and apoptotic assay. Moreover, a molecular docking study was performed to investigate the interaction of some representive compounds with the active site of EGFR- TK.

Keywords: Quinazoline, EGFR, MCF-7, A549, WI38, Apoptosis

*Corresponding author: Heba Abdelrasheed Allam

E-mail: hebaallam80@hotmail.com ; Tel: +201006377655.

1. Introduction

Cancer is a malignant life-threatening disease which stands next to cardiovascular diseases in terms of morbidity and mortality and is projected to be the primary cause of death worldwide in the future.[1] The discovery of effective safe new anticancer agent is still a serious research field due to the side effects of the conventional non-selective cytotoxic chemotherapies, their systemic toxicity and resistance.[2,3] Targeted therapies selectively aim cancer cells or the tumor microenvironment that supports cancer growth with higher effectiveness and slight off-target side effects on normal cells.[3] Targeted chemotherapies specifically attack signaling pathways regulating tumor cell cycle and its microenvironment prompting cell apoptosis, delaying tumor cell proliferation and/or obstructing tumor mass growth.[4,5] Epidermal growth factor receptor (EGFR) signaling pathway has been extensively investigated for its significant role in the progression of different types of malignant tumors, where development of small molecules targeting EGFR is a well-known strategy for design of antitumor agents.[6] Many reports referred to the pivotal role of quinazoline derivatives as selective and potent EGFR inhibitors along with their remarkable antitumor activity.[7–9] Reviewing the literature revealed that certain monosubstituted quinazolines, namely: 4-(3-bromo / chloroanilino)quinazolines **1** and **2** exert a significant EGFR inhibition.[10,11] Also, the disubstituted quinazolines: 4-(7-amino-2-aryl)-2-(4-fluorophenyl)-5-bromoindolequinazolines **3a,b** show good cytotoxicity against **A549**, **MCF-7** and **HeLa** cell lines, in addition to their nanomolar EGFR inhibitory activity.[12] Furthermore, 2,4,6-trisubstituted quinazoline **4,** displays a significant anticancer activity against different subpanel tumor cell lines with GI_{50} value 16.9 μM.[13] (Figure 1)

Accordingly, we design a series of novel 2,4,6-trisubstituted quinazoline derivative by keeping the disubstituted 4-amino quinazoline scaffold in **3a,b** and bioisosteric replacement of their indolyl and 2-phenyl moieties with benzothiazolyl and pyridin-3-yl ones, respectively. In addition, introduction of bromo group at position **6** is carried out to obtain compounds **VIIa-c**. Moreover, guided by the significant anticancer activity of the trisubstituted quinazoline derivative **4** compounds **XIa-c** were designed via retaining NH linker at position 4 and replacing of methyl benzene sulfonamide moiety by amido moieties, bioisosteric replacement of thien-2-yl with pyridin-3-yl and substitution of 6-iodo with 6-bromo aiming to obtain new derivatives with promising anticancer and EGFR inhibitory activities. Further modification includes bioisosteric substitution of NH at position 4 with O to give **VIIIa-f** in order to inspect the effect of this substitution on the designed biological activity. The extended side chain of **lapatinib 5** at position 4 directed our interest to synthesize series **IXa-d** hoping to improve the anticancer and EGFR inhibitory activities of the newly prepared quinazolines.

Another approach deals with NH spacer elongation at position 4 to NH NH CO and NH N=CH to produce 4-substituted benzohydrazides **XIIa-c** and 4-substituted arylideneaminoquinazolines **XIVa-i**.

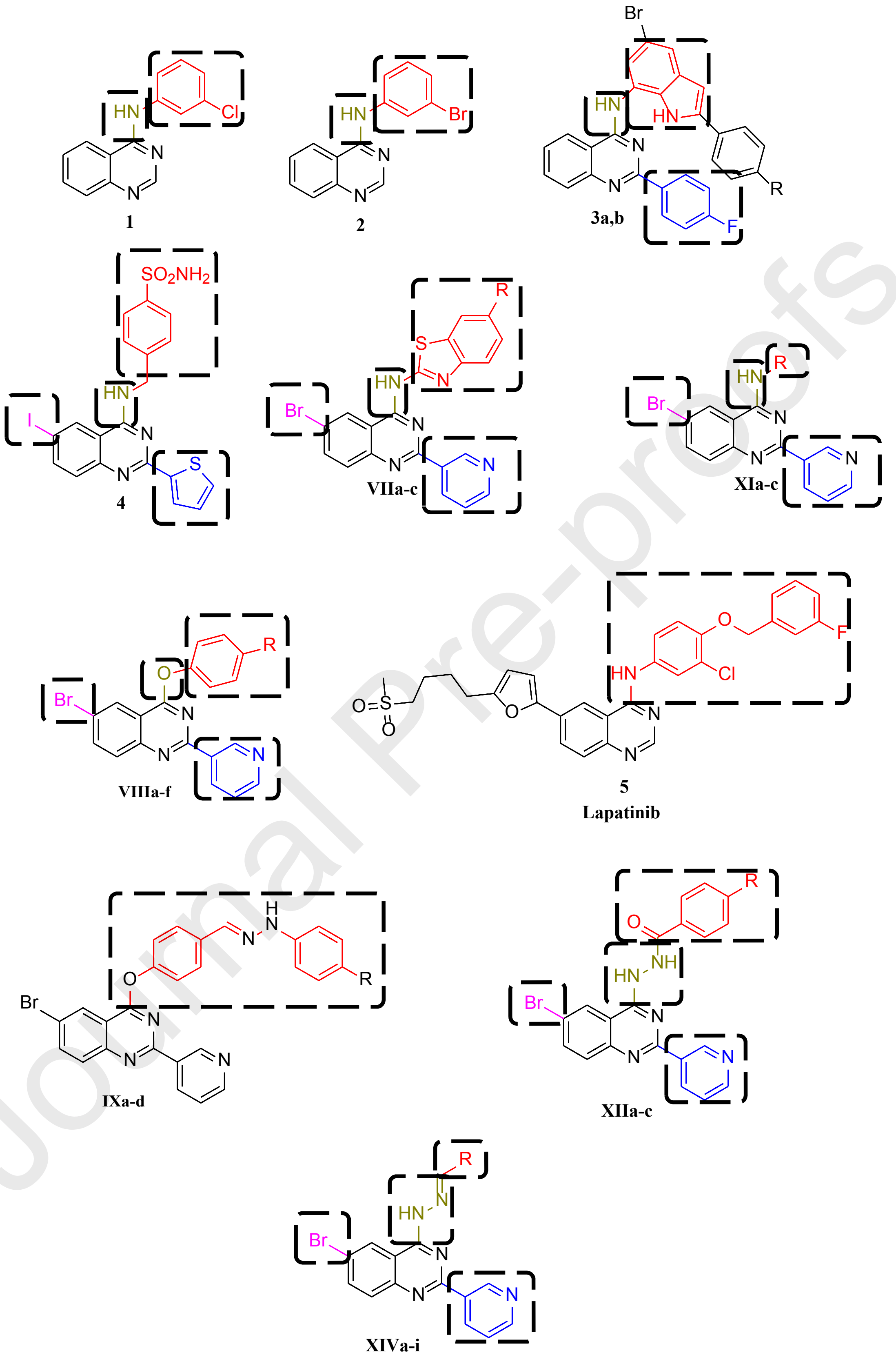

Fig. 1: Reported quinazoline anticancer agents, and the scaffold of the target compounds

2. Results and discussion

2.1. Chemistry

The synthetic pathways implemented for the synthesis of the intermediates and target quinazolines are shown in **Schemes 1 - 4**. Reaction of 2-aminobenzoic acid with Br_2 in refluxing glacial acetic acid afforded 5-bromoanthranilic acid which upon reaction with freshly prepared nicotinoyl chloride gave the amidated intermediate **III**. Reflux of **III** with acetic anhydride produced the benzoxazinone **IV**. Heating of **IV** under reflux with formamide resulted in quinazolinone **V**, which upon reflux with $POCl_3$ afforded 4-chloro derivative **VI**. Reaction of **VI** under reflux with the appropriate 2-amino-6-un/substituted benzothiazoles in dimethylformamide and in presence of anhydrous potassium carbonate produced **VIIa-c**, while reaction of **VI** at room temperature with the appropriate phenolic compounds in dimethylformamide and in presence of anhydrous potassium carbonate gave **VIIIa-f. Scheme 1**. IR spectra of compounds **VIIa-c** showed the appearance of NH bands at 3394 – 3369 cm^{-1}. ^{1}H-NMR spectra of **VIIa**, **VIIb** and **VIIc** exhibited D_2O exchangeable singlet signals at 8.76, 8.68 and 8.67 ppm, respectively, corresponding to NH proton. In addition, a (triplet quartet) pattern was observed at 1.38 and 4.00 ppm for compound **VIIb** corresponding to ethoxy protons. ^{13}C-NMR spectrum of **VIIb** revealed two aliphatic signals at 15.19 and 64.04 attributed to $\underline{C}H_3$ and $\underline{C}H_2$ of ethyl carbons, respectively. IR spectrum of **VIIId** revealed three strong bands at 2819, 2792 and 1693 cm^{-1}, assignable for the aldehydic H and C=O groups, respectively, while that of **VIIIf** elicited two strong bands at 3251 and 1670 cm^{-1}, attributed to the NH and C=O groups of respectively. ^{1}H-NMR spectra revealed the presence of a singlet signal at 2.4 ppm integrated for the three protons of the methyl group of **VIIIb**, a singlet signal at 10.09 ppm due to the proton of the aldehydic group of **VIIId** and a singlet signal at 2.1 ppm and a D_2O exchangeable singlet signal at 10.11 ppm integrated for the methyl group and NH protons of **VIIIf**, respectively.

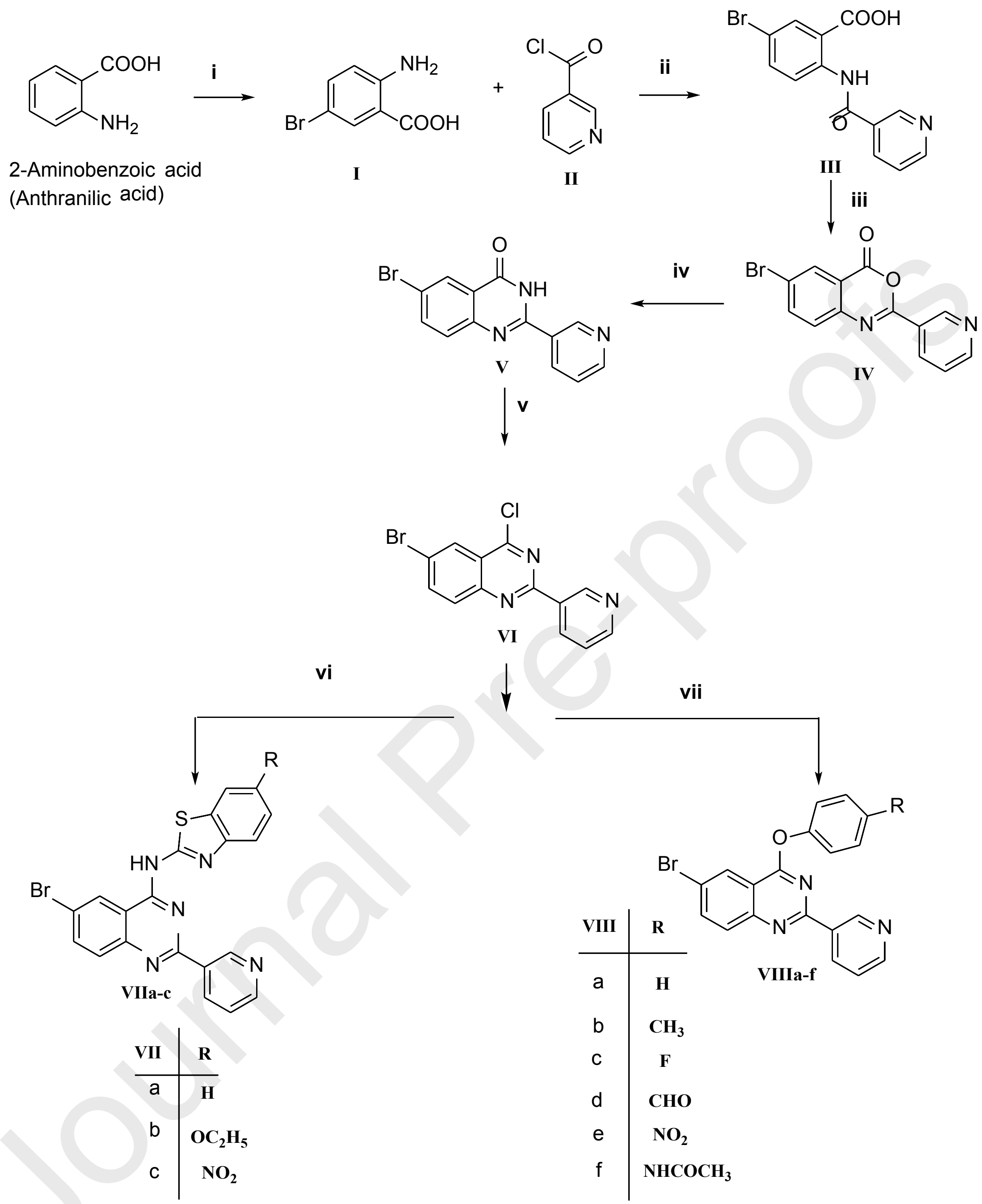

Scheme 1: Synthesis of the intermediates **I, II, III**, **IV**, **V, VI** and the target compounds **VIIa-c and VIIIa-f**; Reagents and conditions: (**i**) Br_2, glacial acetic acid, ice bath; (**ii**) Methylene chloride, triethylamine, 24 h RT; (**iii**) Acetic anhydride, reflux 4.5 h; (**iv**) Formamide, reflux 2.5 h; (**v**) $POCl_3$, reflux 2.5 h; (**vi**) appropriate 2-amino benzothiazole derivatives, DMF, anhyd. K_2CO_3, reflux 9 h; (**vii**) (un)substituted phenol derivatives, DMF, anhyd. K_2CO_3, stirr on cold 24 h.

Reaction of compound **VIIId** with the appropriate un/substituted phenyl hydrazines in absolute ethanol and in presence of few drops of glacial acetic acid furnished the target compounds **IXa-d**. **Scheme 2**. Structures assigned to the products were deduced from concordant microelemental and spectral analyses. IR spectra of compounds **IXa-d** showed presence of a sharp band corresponding to NH groups at 3221 – 3313 cm^{-1}. IR spectrum of compound **IXd** revealed a forked band at 3421 and 3331 cm^{-1} corresponding to NH_2 group, in addition to two bands attributed to SO_2 group at 1319 and 1141 cm^{-1}. ^{1}H-NMR spectra of compounds **IXa-d** showed an increase in the integration of the aromatic protons indicating the presence of additional aromatic ring, in addition to the absence of singlet signal of the aldehydic proton along with the appearance of a sharp singlet signal around 7.91 – 8.05 ppm corresponding to azomethine proton together with the appearance of a D_2O exchangeable singlet signal around 10.30 – 10.90 ppm corresponding to NH proton. Compound **IXc**, displayed a singlet signal at 3.70 ppm attributed to OCH_3 protons. NH_2 protons of compound **IXd** appeared as a singlet signal at 7.09 ppm which disappeared upon deuterium exchange.

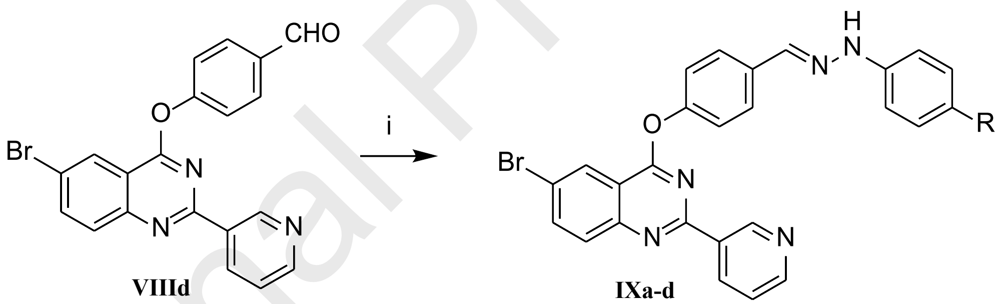

VIIId **IXa-d**

IX	R
a	**H**
b	**Cl**
c	**OCH_3**
·	**SO_2NH_2**

Scheme 2: Synthesis of the target compounds **IXa-d** from the target compound **VIIId**; Reagent and condition: (**i**) absolute ethanol, drops of glacial acetic acid, phenylhydrazine/4-hydrazinylbenzenesulfonamide, reflux 9.5-15 h. 4-chlorophenylhydrazine/4-methoxyphenylhydrazine, stirr on cold 24 h.

Additionally, 4-hydrazino derivative **X** was produced by reflux of quinazolinone **VI** with hydrazine hydrate. Heating of **X** under reflux with appropriate acid anhydride gave the corresponding compounds **XIa-c,** whereas treatment of **X** with appropriate p-substituted benzoyl chlorides in methylene chloride and in presence of trimethylamine at room temperature resulted in compounds **XIIa-c** as shown in **Scheme 3.** The structure **X** was supported by analytical and spectral data. IR spectrum displayed the appearance of the characteristic stretching vibrations of the hydrazinyl moiety at 3300, 3294 and 3209 cm^{-1}. ^{1}H-NMR spectrum showed two singlet signals at 5.02 and 9.86 ppm, which disappeared on deuteration, corresponding to the NH_2 and NH, respectively. IR spectra of compounds **XIa-c** showed two bands attributed to the two carbonyl groups at 1732 – 1714 cm^{-1}. ^{1}H-NMR spectra of **XIa-c** lacked the NH_2 protons signal at 5.02 ppm along with the appearance of aliphatic signal at 3.03 ppm corresponding to the -CH_2-CH_2- protons of **XIa**, in addition to an increase in the integration of aromatic protons of compound **XIc**, while **XIb** spectrum indicated the presence of a singlet signal at 2.45 ppm corresponding to the methyl protons of the diacetyl moiety. ^{13}C-NMR spectra of **XIa,b,c** showed a signal at 185.20, 172.49 and 166.42 ppm attributed to the two additional equivalent carbonyl groups, respectively. IR spectra of **XIIa-c** displayed the disappearance of the characteristic stretching vibrations of the NH_2 moiety of **X** and revealed the appearance of new band at 1643, 1645 and 1658 cm^{-1} related to the new carbonyl group of the benzohydrazides; **XIIa, XIIb** and **XIIc**, respectively. ^{1}H-NMR spectra of **XIIa-c** lacked the NH_2 protons signal at 5.02 ppm and showed D_2O exchangeable protons at 10.68 - 11.13 ppm corresponding to the NH protons, in addition to an increase in the aromatic integration. Compound **XIIb** revealed an extra aliphatic singlet signal at 3.88 ppm related to the CH_3 protons.

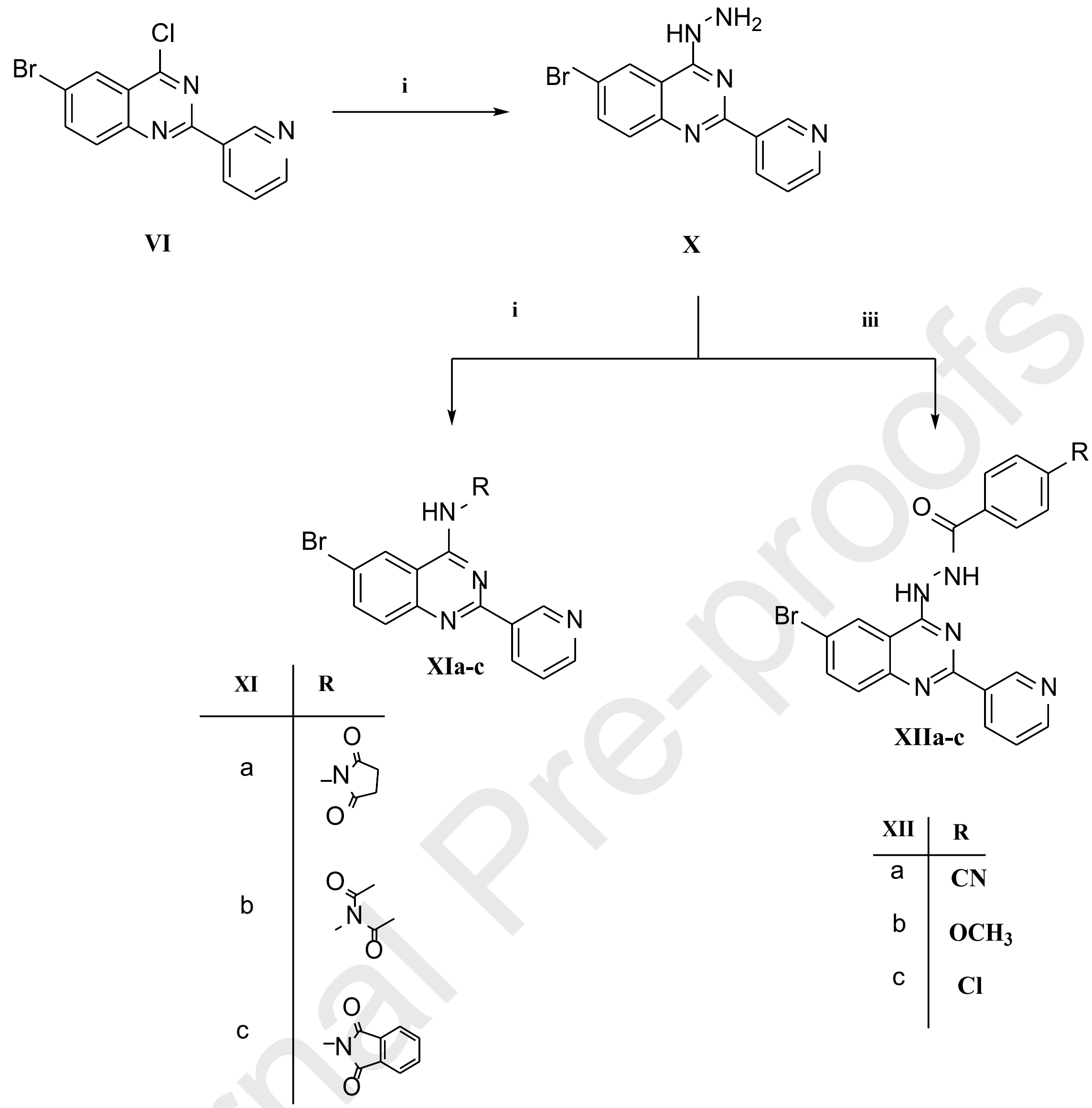

Scheme 3: Synthesis of the new intermediate compound **X**, the target compounds **XIa-c** and **XIIa-c**; Reagents and conditions: (**i**) NH_2NH_2 99%, reflux 8.5 h; (**ii**) acid anhydride, glacial acetic acid, reflux 4-13 h; (**iii**) appropriate 4-substitutedbenzoylchloride, methylene chloride, triethylamine, stirr on cold 10-72 h.

Finally, the target compounds **XIVa-i** were gained via condensation of 4-hydrazino derivative **X** with appropriate aldehydes in absolute ethanol under reflux as displayed in **Scheme 4**. The expected structures of compounds **XIVa-i** were confirmed by IR spectra that displayed the presence of the characteristic stretching vibration of NH group in the range of 3448 - 3394 cm^{-1}. ^{1}H-NMR spectra of compounds **XIVa-i** revealed an increase in the integration of the aromatic protons indicating the presence of additional aromatic ring, in addition to the appearance of a singlet signal around 11.70 - 12.20 ppm corresponding to the NH proton which disappeared upon deuterium exchange. Additionally, compound **XIVc** showed a singlet signal at 2.70 ppm corresponding to OCH_3 protons. The morpholinyl protons of **XIVg** appeared as two triplets at 3.25 and 3.77 ppm. Compound **XIVh** displayed a singlet signal at 2.23 ppm assigned to $\underline{CH_3}$ piperazinyl protons along with two triplet signals at 2.46 and 3.28 ppm of the piperazinyl protons. ^{13}C-NMR spectra of **XIVc** showed a signal at 55.84 ppm attributed to the $O\underline{C}H_3$ carbon.

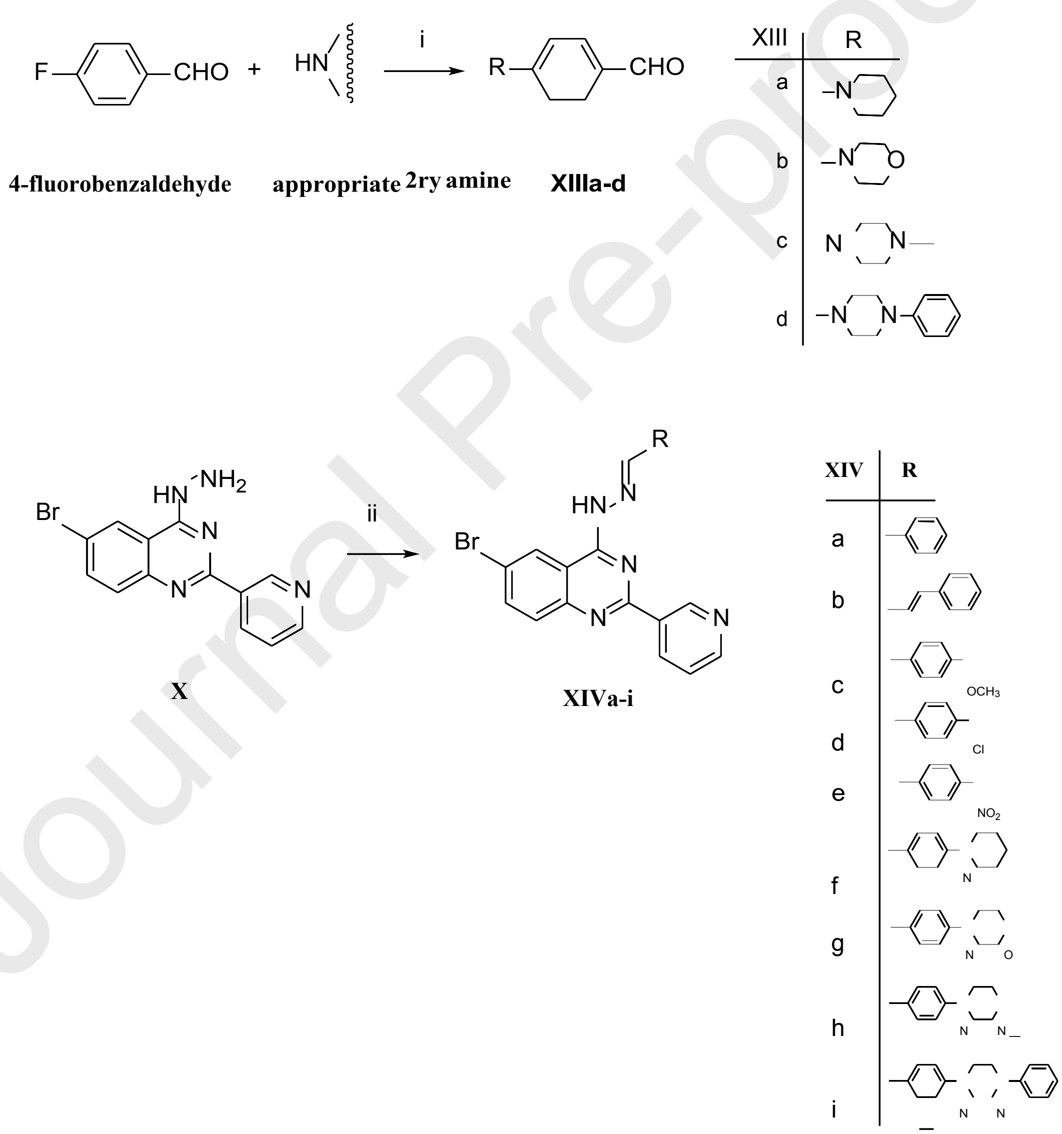

Scheme 4: Synthesis of reported aldehydic reagents **XIIIa-d** and the target compounds **XIVa-i**; Reagents and conditions: (**i**) DMF, anhyd. K_2CO_3, reflux 6-7 h; (**ii**) appropriate aldehyde, absolute ethanol, reflux 10-17 h.

2.2. Biological evaluation

All the newly synthesized compounds were subjected to EGFR-TK inhibitory assay and most active ones were screened for their *in vitro* cytotoxicity against two cancer cell lines, namely; the non-small cell lung cancer cell line **A549** and breast cancer cell line **MCF-7**, in addition to normal fibroblast cell line **WI38**. Compounds showed promising inhibitory activity against wild-type EGFR were evaluated for their inhibitory activity on mutant EGFR and their *in vitro* cytotoxicity against two cancer cell lines expressing mutant EGFR, namely, **PC9** and **HCC827**. Furthermore, a representative compound eliciting superior EGFR inhibition was subjected to cell cycle analysis and apoptotic assay to investigate its effect on the cell cycle progression and the apoptosis percentage induced by this compound.

2.2.1. EGFR - TK inhibitory assay:

All the newly target compounds **VIIa-c**, **VIIIa-f**, **IXa-d**, **XIa-c**, **XIIa-c** and **XIVa-i** were inspected *in vitro* for their EGFR inhibitory activity. **Table 1** shows the inhibition data (IC_{50} values) of the examined compounds and **Gefitinib**, as a reference standard, towards EGFR. As presented in **Table 1**, all the tested compounds showed EGFR inhibitory activity with IC_{50} values ranging from sub micromolar to single-digit micromolar concentration (0.096 – 2.962 μM).

The obtained results showed that twenty-four compounds out of twenty-eight exhibited superior activities at sub-micromolar level (IC_{50}= 0.096 - 0.818 μM) as EGFR inhibitors compared to **Gefitinib** (IC_{50}= 0.166 μM). Three compounds: 4-(6-unsubstituted benzothiazole) **VIIa**, 4-acetamido phenoxy **VIIIf** and 4-nitrobenzylidene **XIVe** quinazoline derivatives demonstrated comparable enzyme inhibitory activity (IC_{50}= 0.096, 0.149 and 0.141 μM, respectively) to that expressed by **Gefitinib** (IC_{50}= 0.166 μM). The spacer variation at position 4 with **NH**, **O**, **NH-N=CH** or **NH-NH-C=O** gave compounds with promising EGFR inhibitory activity at sub-micromolar level. This indicated that alteration of the spacer does not greatly affect the EGFR inhibition. These three compounds were further tested against mutant EGFR kinases (**T790M** and **L858R**) and their results are shown in **Table 2**. The results showed that compound **VIIa** and

XIVe have comparable activity to **Gefitinib** against the mutated type **T790M,** and compound **VIIIf** was comparable to **Gefitinib** against the mutated type **L858R.**

Table 1: EGFR inhibitory activity of the target compounds compared to **Gefitinib** as a reference standard.

Cpd. No.	**EGFR IC_{50} (µM)**	**Cpd. No.**	**EGFR IC_{50} (µM)**	**Cpd. No.**	**EGFR IC_{50} (µM)**
VIIa	0.096 ± 0.00278	**IXb**	0.431±0.01241	**XIVb**	0.258 ± 0.00992
VIIb	0.454 ± 0.01309	**IXc**	0.303±0.00874	**XIVc**	0.573 ± 0.01651
VIIc	0.339 ± 0.01303	**IXd**	0.231±0.0087	**XIVd**	0.296 ± 0.01138
VIIIa	0.483 ± 0.01391	**XIa**	1.748 ± 0.06714	**XIVe**	0.141 ± 0.00408
VIIIb	0.818 ± 0.02356	**XIb**	0.461 ± 0.01771	**XIVf**	0.183 ± 0.00527
VIIIc	1.983 ± 0.07618	**XIc**	0.331 ± 0.01274	**XIVg**	0.289 ± 0.01111
VIIId	0.728 ± 0.0279	**XIIa**	0.303 ± 0.00874	**XIVh**	1.246 ± 0.04785
VIIIe	0.660 ± 0.01902	**XIIb**	0.292 ± 0.00843	**XIVi**	0.282 ± 0.00812
VIIIf	0.149 ± 0.00429	**XIIc**	0.286 ± 0.01099	**Gefitinib**	0.166 ± 0.00638
IXa	2.962 ± 0.11374	**XIVa**	0.796 ± 0.03058		

Table 2: Mutant EGFR inhibitory activity of the target compounds compared to **Gefitinib** as a reference standard.

Cpd. No.	**IC_{50} (uM)**	
	$EGFR_{T790M}$	**$EGFR_{L858R}$**
VIIa	0.028±0.00069	0.055±0.00136
VIIIf	0.048±0.00118	0.012±0.00029
XIVe	0.025±0.00061	0.042±0.00103
Gefitinib	0.023±0.00057	0.018±0.00045

2.2.2. In vitro cytotoxic activity:

After being investigated for their EGFR inhibitory activity, Fifteen compounds **VIIa,c, VIIIf, IXc,d, XIc, XIIa-c** and **XIVb,d-g,i** out of the twenty eight newly synthesized compounds that elicited superior to good EGFR inhibitory activity (0.096-0.339 µM) were selected to be evaluated for their *in vitro* cytotoxicity against two EGFR-overexpressing cell lines, *viz*, the non-small cell lung carcinoma cell line **A549** which is well-known to overexpress wild-type EGFR [14,15] and the breast cancer cell line **MCF-7** which is well-known to overexpress various growth factor receptors including wild-type EGFR [16–21] to demonstrate their cellular efficacy. Furthermore, they were evaluated using normal fibroblast cells **WI38** for their cytotoxicity to evaluate the compounds' selectivity towards tumor cells. Additionally, three quinazoline derivatives **VIIa, VIIIf** and **XIVe** that revealed comparable enzyme inhibitory activity (IC50= 0.096, 0.149 and 0.141 µM, respectively) to that expressed by **Gefitinib** (IC50= 0.166 µM) were selected to be evaluated using mutant EGFR-expressing cell lines including **PC9** and **HCC827** (both cell lines carry a Glu746-Ala750 deletion mutation in exon 19) using MTT assay [22]. In this *in vitro* testing, **Gefitinib** was used as a reference standard. The *in vitro* cytotoxic data of the tested compounds are shown in **Table 3.**

Table 3: Cytotoxicity of the tested compounds and **Gefitinib** against **A549, MCF-7, WI38, PC9** and **HCC827** cell lines and the selectivity index **(SI*)** for the tested compounds and **Gefitinib** relative to normal cell line**.**

Cpd. No.	IC_{50} (uM)					Selectivity index (SI)	
	A549	MCF-7	WI38	PC9	HCC827	A549	MCF-7
VIIa	178.34 ± 8.9	2.49 ± 0.12	82.8 ± 4.14	1.05±0.02	3.43±0.066	0.464	33.253
VIIc	24.55 ± 1.22	3.195 ± 0.15	268.8 ± 11.6	NA	NA	10.949	84.131
VIIIf	29.16 ± 1.45	19.03 ± 0.95	57.72 ± 2.88	4.02±0.077	1.21±0.023	1.979	3.033
IXc	6.36 ± 0.21	1.89 ± 0.03	45.53 ± 1.28	NA	NA	7.158	24.089

IXd	5.774 ± 0.28	9.996 ± 0.44	56.80 ± 2.71	NA	NA	9.837	5.682
XIc	28.206 ± 1.41	10.142 ± 0.46	53.86 ± 2.6	NA	NA	1.909	5.310
XIIa	33.961 ± 1.69	6.881 ± 0.34	50.89 ± 2.21	NA	NA	1.498	7.395
XIIb	10.77 ± 0.52	8.22 ± 0.17	21.49 ± 0.92	NA	NA	1.995	2.614
XIIc	10.514 ± 0.52	2.517 ± 0.12	36.57 ± 1.61	NA	NA	3.478	14.529
XIVb	9.151 ± 0.45	11.879 ± 0.51	40.20 ± 1.84	NA	NA	4.393	3.384
XIVd	63.572 ± 3.17	0.956± 0.04	27.69 ± 1.33	NA	NA	0.435	28.964
XIVe	3.50 ± 0.17	20.48 ± 1.02	64.68 ± 3.23	3.66±0.071	5.49±0.11	18.480	3.158
XIVf	12.31 ± 0.61	56.50 ± 2.82	63.26 ± 3.16	NA	NA	5.139	1.119
XIVg	5.585 ± 0.27	45.559 ± 2.14	70.32 ± 3.34	NA	NA	12.590	1.543
XIVi	2.47 ± 0.06	8.42 ± 0.24	20.92 ± 0.77	NA	NA	8.469	2.484
Gefitinib	4.389 ± 0.21	4.972 ± 0.24	34.95 ± 1.72	1.36±0.02	3.99±0.07	7.963	7.029

SI* = activity of the tested compounds (IC_{50}) against normal cell line (WI38)/activity of the tested compounds (IC_{50}) against cancer cell line.
NA = not determined

The results presented in **Table 3** revealed that, most of the tested compounds showed a selective anticancer activity against **MCF-7** rather than **A549** cell line. Two compounds **XIVe** and **XIVi** elicited promising anticancer activity against **A549** with IC_{50} of 3.50 and 2.47 µM, respectively, relative to **Gefitinib** (IC_{50}= 4.39 µM). Five compounds **VIIa, VIIc, IXc, XIIc** and **XIVd** displayed a superior anticancer activity against **MCF-7** with IC_{50} of 0.096 – 3.19 µM) compared to **Gefitinib** (IC_{50}= 4.97 µM). 4-(4-Phenylpiperazin-1-yl)benzylidenehydrazinyl **XIVi** was the most potent quinazoline derivative against

A549 lung carcinoma cell line with IC_{50} of 2.47 μM, whereas, the 4-chlorobenzylidenehydrazinyl **XIVd** congener was the most active compound against **MCF-7** with IC_{50} of 0.956 μM. Twelve compounds **VIIa, VIIc, VIIIf, IXc, IXd, XIc, XIIa, XIIc, XIVb, XIVe, XIVf** and **XIVg** out of fifteen displayed low cytotoxicity against the normal fibroblast cells **(WI38)** with good selectivity index.

Among the selected compounds for evaluation against EGFR-dependent cell lines **PC9** and **HCC827**, compound **VIIa** was better than **Gefitinib** against the two cell lines. Whereas, Compound **VIIIf** was superior than **Gefitinib** on **HCC827** cell line.

2.2.3. Cell Cycle Analysis:

The unsubstituted benzothiazol-2-amine **VIIa** that showed a superior EGFR inhibition and anticancer activity against **MCF-7** cell line was subjected to cell cycle analysis and apoptotic assay in order to investigate its effect on cell cycle progression and the apoptosis percentage induced by the compound.

The results of the cell cycle analysis of compound **VIIa** are shown in **Table 4** and **Figure 2**.

Table 4: Cell cycle analysis results of compound **VIIa** after 24 h in **MCF-7** cell line.

Cpd. No.	%G0-G1	%S	%G2/M	%Pre-G1	Comment
VIIa	27.29	31.25	41.45	24.19	Pre G1 apoptosis and Cell growth arrest at G2/M.
Control	53.89	39.01	7.1	1.47	

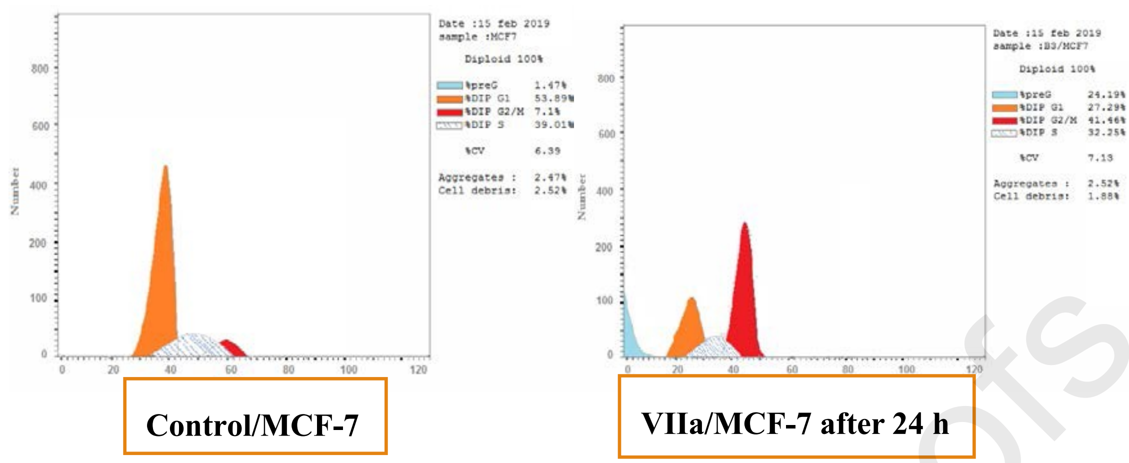

Fig. 2. Effect of compound **VIIa** on the cell cycle of **MCF-7** cells after 24 h.

The results obtained from **Table 4** and **Figure 2** revealed that compound **VIIa** led to pre G1 apoptosis with cell growth arrest at G2/M phase in **MCF-7** cells after 24 h which was confirmed by an increase in the percentage of DNA content (41.46 %) after addition of the compound compared to the control cells (7.1 %).

2.2.4. Apoptotic Assay:

To investigate the apoptosis induction effect and to quantify the percentage of apoptosis induced by compound **VIIa** in **MCF-7** cells, Annexin V-FITC/propidium iodide dual staining assay was carried out according to the reported method [23,24]. The Annexin V assay offers the possibility of identifying early phases of apoptosis before the loss of cell membrane integrity and permits measurements of the kinetics of apoptotic death in relation to the cell cycle.

The effect of compound **VIIa** on apoptotic induction in **MCF-7** cells are shown in **Table 5** and **Figure 3**.

Table 5: Effect of compound **VIIa** on apoptotic induction compared to the control cells after 24 h.

Cpd. No.	Apoptosis			Necrosis
	Total	Early	Late	
VIIa / MCF7	24.19 %	6.27 %	15.64 %	2.28 %
Control /MCF7	1.47 %	0.87 %	0.26 %	0.34 %

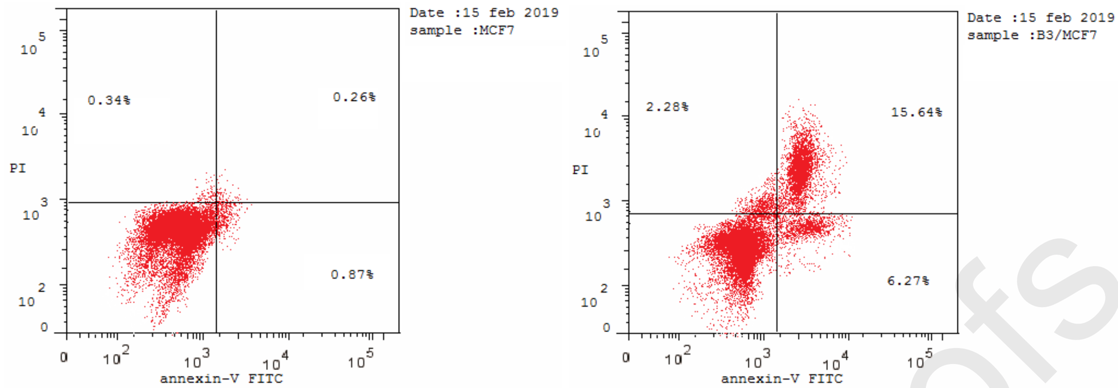

Control/MCF-7 **VIIa/MCF-7 after 24 h**

Fig. 3. Effect of compound **VIIa** on apoptosis induction of **MCF-7** cells after 24h.

The results obtained from **Table 6** and **Figure 3** demonstrated that the percentage of the total apoptotic cells in **MCF-7** cell line increases after treatment with compound **VIIa** (24.19 %) relative to control cells (1.47 %) which represents a prominent marker of apoptosis. The quinazolin-4-yl-(6-unsubstituted benzothiazol-2-amine) **VIIa** revealed cell growth arrest at G2/M phase, in addition to its apoptotic induction effect.

2.3. Molecular Modeling Study

2.3.1. Molecular docking study:

Molecular docking simulations were performed for compounds **VIIa**,**c**, **VIIIf**, **IXb**, **XIc**, **XIIb** and **XIVe** eliciting significant EGFR inhibitory activity in order to investigate their binding mode in the EGFR active site using the X-ray crystallographic structure of EGFR co-crystallized with the 4-anilinoquinazoline derivative **Lapatinib** (PDB ID: 1XKK). The molecular docking setup was first validated by carrying out self-docking of **Lapatinib** in the EGFR active site. The re-docking validation step reproduced the experimental binding mode of the co-crystallized ligand precisely demonstrating that the used docking protocol is suitable for the intended docking study. This is shown by the small RMSD between the docked pose and the co-crystallized ligand (1.63 Å); the energy score (S) = −15.11 kcal/mol and the ability of the docking pose to reproduce all the key interactions attained by the co-crystallized ligand with the hot spots in the active sites; H-bonding with Met793 and through water mediated H-bonding with Thr854 as shown in **Figure 4 and 5**. The validated setup was then used in expecting the ligands receptor interactions at the binding site for the compounds of interest.

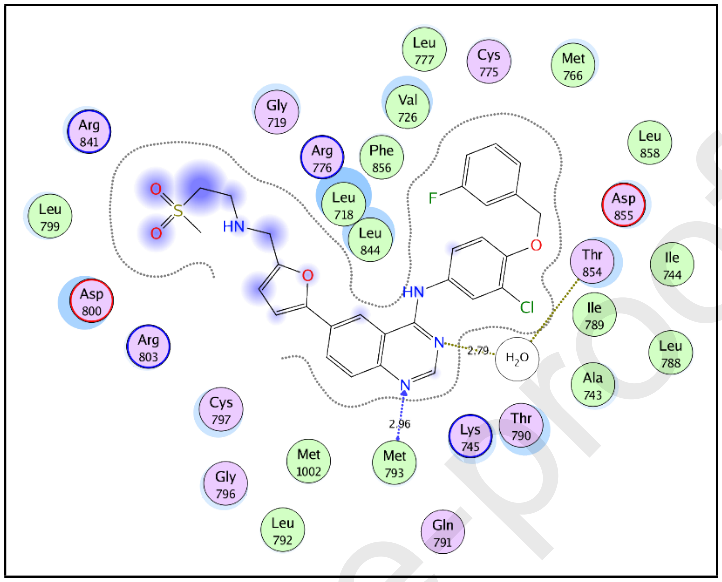

Fig. 4. 2D interaction diagram showing **Lapatinib** docking pose interactions with the key amino acids in the EGFR binding site.

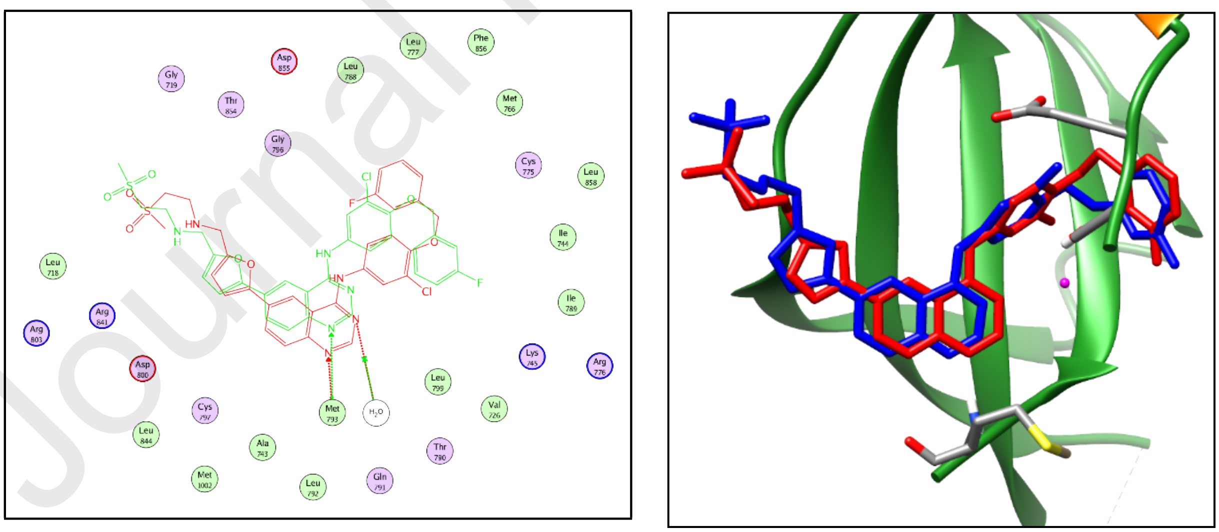

(a) **(b)**

Fig. 5. 2D diagram **(a)** and 3D representation **(b)** of the superimposition of the co-crystallized (red) and the docking pose (blue) of **Lapatinib** in the EGFR binding site with RMSD of 1.63Å. (ligand hydrogen atoms were removed for clarity)

The experimentally used reference **Gefitinib** showed the same binding pattern as **Lapatinib** as displayed in **Figure 6**.

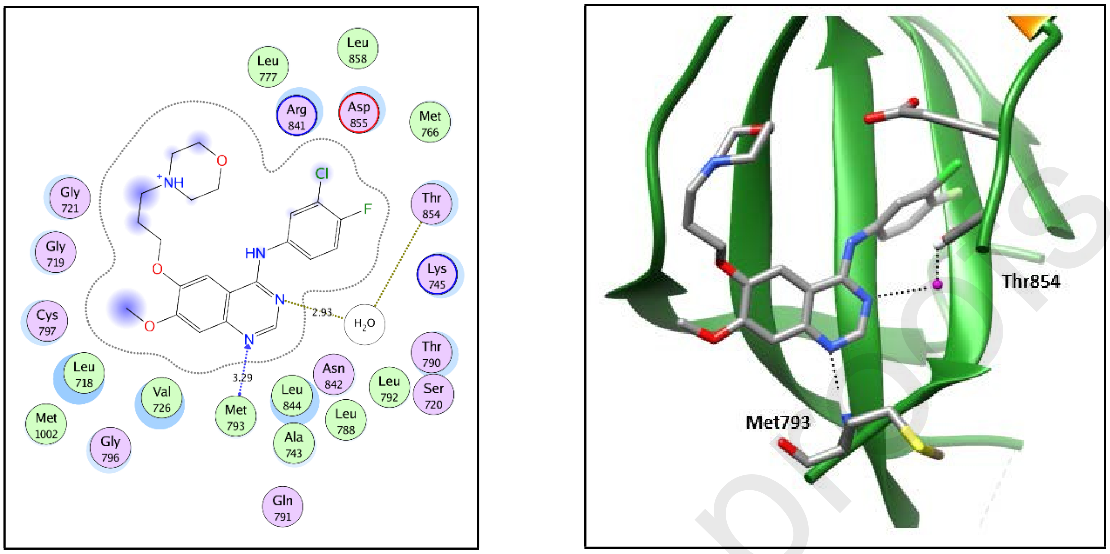

(a) **(b)**

Fig. 6. 2D diagram **(a)** and 3D representation **(b)** of **Gefitinib** in the EGFR binding site.

According to the performed docking study, the most active compounds **VIIa,c**, **VIIIf**, **IXb**, **XIc**, **XIIb** and **XIVe** show a common expected binding pattern in the ATP binding site as shown in **Figure 7-9**. They form a water-mediated hydrogen bond with the key amino acid Thr854 backbone NH by their nitrogen atom at position **1** of the quinazoline ring and H-bond with the key amino acid Met793 by their nitrogen atom in 2-pyridin-3-yl. In addition to the interactions with the key amino acids, they achieve further interactions with the ATP binding site, where they interact by their amino group at position **4** of the quinazoline ring through hydrogen bonding with the COO^{-} moiety of Asp855 and through hydrophobic interaction *via* the bromo group at position **6** of the quinazoline ring with the hydrophobic side chains of the amino acids Met766, Leu788 and Leu858. **Table 6** shows their docking scores**.** The binding pattern of these compounds explains their superior EGFR inhibitory activity as revealed by their experimental EGFR inhibitory assay results as presented in **Table 1** and their binding affinity (docking score) relative to the reference **Gefitinib** as displayed in **Table 6**.

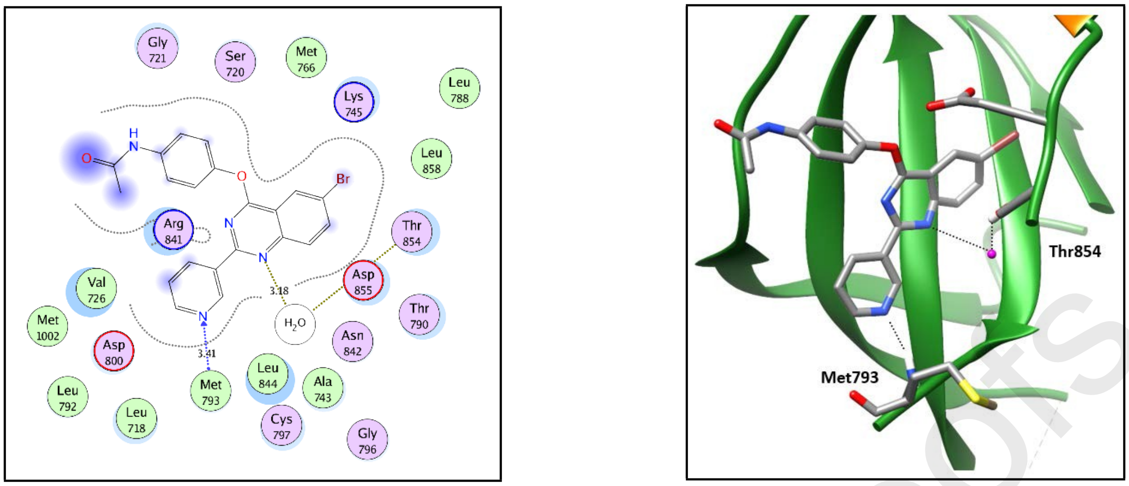

(a) **(b)**

Fig. 7. 2D diagram **(a)** and 3D representation **(b)** of compound **VIIIf** in the EGFR binding site.

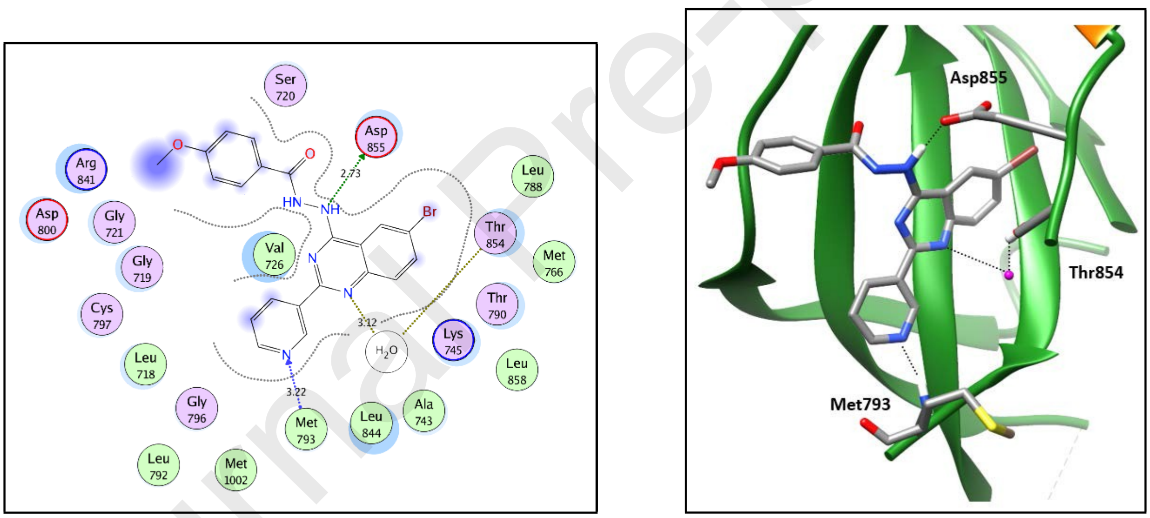

(a) **(b)**

Fig. 8. 2D diagram **(a)** and 3D representation **(b)** of compound **XIIb** in the EGFR binding site

The most potent compound **VIIa** shows a different expected binding pattern in the ATP binding site as shown in **Figure 9**. It forms a H-bond with the key amino acid Met793 by the nitrogen atom in the pyridyl ring which is attached to the quinazoline ring at position **2.** In addition, the amino group at position **4** of the quinazoline interacts with the COO^{-} moiety of Asp855 through hydrogen bonding. Uniquely, it inserts its benzothiazole bicyclic scaffold in the hydrophobic sub-pocket surrounded by the hydrophobic side chains of the amino acids Ala743, Met766, Leu777, Leu792 and Phe856. This unique binding pattern rationalizes its higher activity. (For further details see SI)

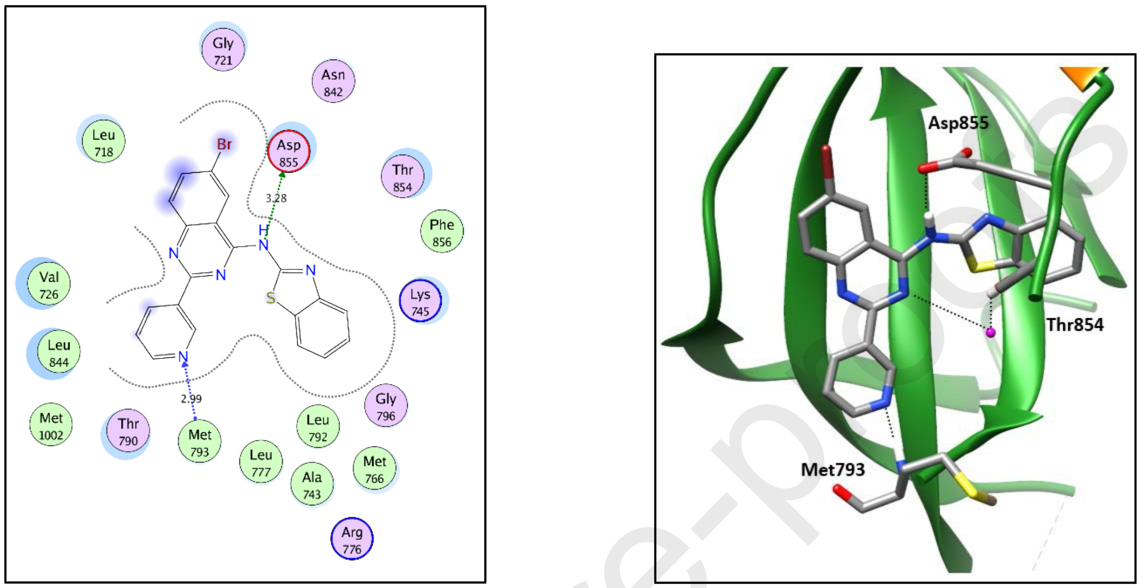

(a) **(b)**

Fig. 9. 2D diagram **(a)** and 3D representation **(b)** of compound **VIIa** in the EGFR binding site.

Table 6: Docking energy scores (*S*) in kcal/mol, interacting amino acid, Distances in Å, H-bond energies in kcal/mol of the tested compounds, **Gefitinib** and **Lapatinib** and their EGFR inhibitory activity (IC_{50} µM).

Compound	**Docking score (*S*) (kcal/mol)**	**Interacting moiety**	**Distances (Å)**	**H-bond energies (kcal/mol)**	**EGFR IC_{50} (µM)**
VIIa	−12.74	Asp855 Met793	3.28 2.99	−1.6 −4.3	0.096
VIIc	−12.34	Asp855 H_2O Met793	2.80 3.13 3.22	−5.7 −1.4 −3.7	0.339
VIIIf	−11.49	H_2O	3.18	−1.2	0.149

		Met793	3.41	−2.3	
IXb	−10.49	Met793	2.80	−3.8	0.431
XIc	−13.00	Asp855 H_2O Met793	2.70 3.14 3.31	−6.4 −1.4 −3.1	0.331
XIIb	−12.44	Asp855 H_2O Met793	2.73 3.12 3.22	−6.2 −1.5 −3.8	0.292
XIVe	−12.38	Asp855 H_2O Met793	2.78 3.14 3.34	−5.9 −1.4 −2.9	0.141
Gefitinib	−12.89	H_2O Met793	2.93 3.29	−1.1 −3.6	0.166
Lapatinib	−15.12	H_2O Met793	2.79 2.96	−1.4 −5.4	NA*

NA* = Not available.

2.3.2. Physicochemical, ADME and pharmacokinetic properties prediction:

SwissADME online web tool provided by the Swiss Institute of Bioinformatics (SIB) is applied for the computation of the physicochemical properties in addition to the prediction of the ADME parameters, pharmacokinetic properties and drug-like nature of the selected compounds **VIIa,c**, **VIIIf**, **IXb**, **XIc**, **XIIb** and **XIVe**. This was carried out to assure that they are not only hopeful candidates in terms of biological efficacy, but also from the pharmacokinetic characteristics. The submitted compounds are predicted to possess promising physicochemical and pharmacokinetic properties. They exhibit a predicted wlogP in a range of 3.51 – 7.16, moderate water solubility, high GIT absorption with no BBB permeability and so no predicted CNS adverse effects. **Figure 10** demonstrates the BOILED-Egg graph of the WLOGP vs. TPSA (Topological Polar

Surface Area) for the submitted compounds [20]. All compounds except **VIIc** and **IXb** are placed in the area of human intestinal absorption (HIA) with no BBB permeability. This graph displays also that they are not P-glycoprotein substrates (PGP-), so they are not liable to the efflux mechanism done by this transporter which is used by many tumor cell lines as a drug-resistance mechanism [21]. Although compounds **VIIc** and **IXb** show very promising kinase inhibitory activity, the lipophilicity of **IXb** or the high polar surface area of **VIIc** impede their HIA and so their oral bioavailability. This increases attention in designing kinase inhibitors to the pharmacokinetics of the compound and not only the good activity attained. The anticipated high GIT absorption of these compounds is due to their optimal physicochemical properties found in the suitable physicochemical properties range for oral bioavailability.

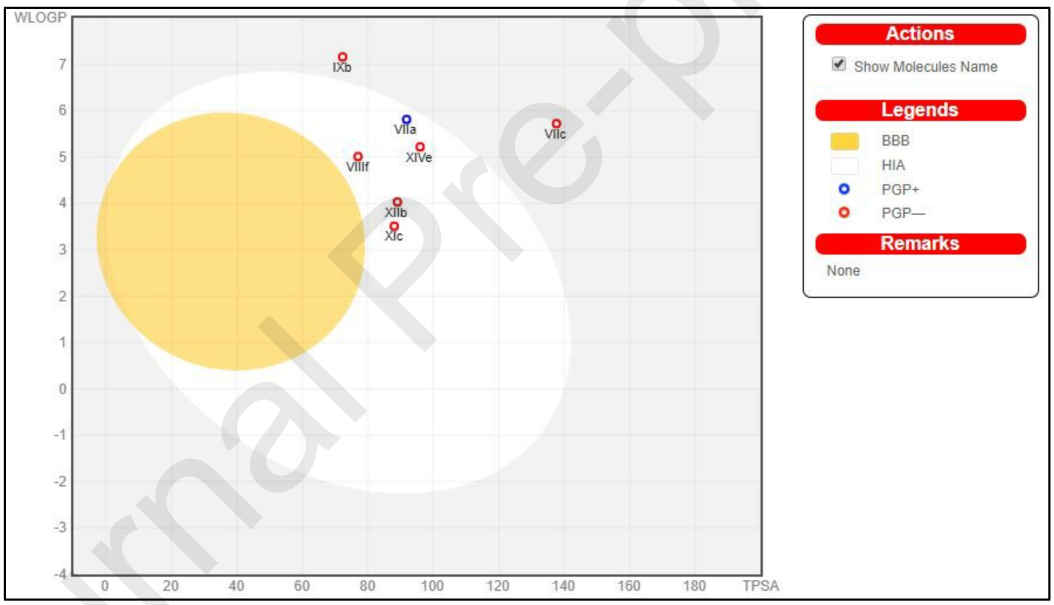

Fig. 10. Predicted Boiled-Egg plot from SwissADME online web tool for compounds **VIIa**,**c**, **VIIIf**, **IXb**, **XIc**, **XIIb** and **XIVe**.

SwissADME online web tool shows also that all the tested compounds except **IXb** (due to its high molecular weight and logP) satisfy the drug-likeness characteristics as defined by the major pharmaceutical companies; Lipinski's (Pfizer) [25], Ghose's (Amgen) [26], Veber's (GSK) [27], Egan's (Pharmacia) [28] and Muegge's (Bayer) [29] filters. However, they are not classified as lead-like as their molecular weights exceeded

350 and most of them is with predicted $\log P_{o/w}$ from XLOGP3 [30] model that is higher than 3.5. In summary, the computational study of the physicochemical and pharmacokinetic properties of the newly synthesized compounds confirms that most of them show promising biological efficiency with hopeful pharmacokinetic properties.

3.Conclusion

Twenty-Eight new compounds were synthesized and evaluated for their EGFR inhibitory activity. Twenty-four compounds exhibited significant wild-type EGFR inhibitory activity at sub-micromolar level (IC_{50}= 0.096 – 0.818 μM) compared to Gefitinib (IC_{50}= 0.166 μM). Fifteen compounds **VIIa,c, VIIIf, IXb,d, XIc, XIIa-c** and **XIVb,d-g,i** that elicit a significant enzyme inhibition were further screened for their anticancer activity against **MCF-7** and **A549** cell lines, in addition to **WI38** normal fibroblast cell line. The majority of the tested compounds showed a selective anticancer activity against MCF-7 rather than A549 cell line. Compounds showed promising inhibitory activity against wild-type EGFR were screened for their inhibitory activity on mutant EGFR ($EGFR_{T790M}$ and $EGFR_{L858R}$) and for their *in vitro* cytotoxicity against two cancer cell lines expressing mutant EGFR, namely, **PC9** and **HCC827**. The most active EGFR inhibitor **VIIa** (IC_{50} = 0.096 μM) was subjected to cell cycle analysis and apoptotic assay. The results of molecular docking study confirmed that the binding mode was consistent with the EGFR inhibitory activity of the tested compounds. Most of the newly synthesized compounds are not only with significant anticancer activity, but also possess promising pharmacokinetic properties.

4. Experimental

4.1. Chemistry:

All chemicals were picked up from commercial suppliers and used without any purification. Reactions were observed by TLC (Kieselgel 60 F254 precoated plates, E. Merck, Germany) and the spots were visualized by exposure to UV lamp at λ 254 nm. Determination of melting points was obtained using Electrothermal Stuart SMP_3 digital melting point apparatus. ^1H NMR and ^{13}C NMR spectra were determined in DMSO-d_6 and recorded on 400 MHz spectrophotometer for ^1H NMR and 100 MHz spectrophotometer for ^{13}C NMR (Bruker AG, Switzerland) at Faculty of Pharmacy, Cairo University; Chemical shift (δ) values are expressed in parts per million (ppm) and coupling constants

(J) in Hertz (Hz). Elemental microanalyses were performed at the Regional Center for Mycology and Biotechnology, Al-Azhar University, Egypt while mass spectra were carried out using Shimadzu Qp-2010 plus Gas Chromatograph-Mass, at the MicroAnalytical Center, Faculty of Science, Cairo University. Infrared Spectra were recorded on Shimadzu-FTIR spectrophotometer, Faculty of Pharmacy, Cairo University, Egypt and expressed in wave number (cm^{-1}), using potassium bromide discs. Compounds **I**, **II** and **XIIIa-d** have been synthesized as reported [31–34].

*4.1.1. 5-Bromo-2-(nicotinamido)benzoic acid **(III)***

Nicotinoyl chloride **II** (2.3 g, 16 mmol) was added to a solution of 5-bromoanthranilic acid **I** (3.5 g, 16 mmol) in methylene chloride (30 ml) and triethylamine (2.26 ml, 16 mmol). The reaction mixture was stirred overnight at room temperature, the obtained solid was filtered, dried and crystallized from ethanol.

White powder, (yield 80%), m.p. 299-300°C; IR (KBr, ν_{max}/cm^{-1}): 3450 - 3425 (OH acid),3406 (NH), 1774 (C=O acid), 1678 (C=O amide), 1593, 1519 (C=C); ^{1}H NMR (DMSO-d_6) δ *ppm*: 7.64 (t, *J*= 6.28 Hz, 1H, Ar-H), 7.86 (dd, *J*= 2.48, 2.48 Hz, 1H, Ar-H), 7.95 (s, 1H, D_2O exchangeable, -NH) , 8.13 (d, *J*= 2.44 Hz, 1H, Ar-H), 8.27 - 8.30 (m, 1H, Ar-H), 8.56 (d, *J*= 8.92 Hz, 1H, Ar-H), 8.83 (dd, *J*=1.16, 1.12 Hz, 1H, Ar-H), 9.12 (d, *J*=1.56 Hz, 1H, Ar-H), 12.17 (s, 1H, D_2O exchangeable, -OH); ^{13}C NMR (DMSO-d_6) δ *ppm*: 115.77, 119.25, 120.77, 123.41, 125.59, 131.41, 133.29, 136.58, 137.09, 139.68, 146.50, 162.97 (C=O amide), 168.77 (C=O acid); MS, *m/z*: 321 [M^+], 323 $[M+2]^+$; Anal. Calcd. % for $C_{13}H_9BrN_2O_3$ (321.13): C, 48.62; H, 2.83; N, 8.72; Found % C, 48.51; H, 3.04; N, 8.96.

*4.1.2. 6-Bromo-2-(pyridin-3-yl)-4H-benzo[d][1,3]oxazin-4-one **(IV)***

A mixture of the amidated anthranilic acid **III** (1.84 g, 5 mmol) in acetic anhydride (15 ml) was heated under reflux for 5 h. Then, the reaction mixture was poured onto ice-water. The obtained solid product was collected by filtration, dried and crystallized from methanol. Off white powder, (yield 65%), m.p. 170-173°C; IR (KBr, ν_{max}/cm^{-1}): 1762 (C=O), 1593, 1519 (C=C); ^{1}H NMR ($CDCl_3$) δ *ppm*: 7.50 (dd, *J*= 4.92, 4.88 Hz, 1H, Ar-H), 7.63 (d, *J*= 8.60 Hz, 1H, Ar-H), 7.97 (dd, *J*= 2.28, 2.28 Hz, 1H, Ar-H), 8.40 (d, *J*= 2.24 Hz, 1H, Ar-H), 8.54 - 8.57 (m, 1H, Ar-H), 8.83 (dd, *J*= 1.36, 1.44

Hz, 1H, Ar-H), 9.52 (d, *J*=1.56 Hz, 1H, Ar-H); ^{13}C NMR (DMSO-d_6) δ *ppm*: 119.40, 121.48, 124.55, 126.45, 129.64, 130.49, 135.85, 140.06, 145.40, 149.09, 153.54, 155.89, 157.86 (C=O); MS, *m/z*: 303 [M$^+$], 305 [M+2]$^+$; Anal. Calcd. % for $C_{13}H_7BrN_2O_2$ (303.12): C, 51.51; H, 2.33; N, 9.24; Found % C, 51.68; H, 2.45; N, 9.41.

4.1.3. 6-Bromo-2-(pyridin-3-yl)quinazolin-4(3H)-one ***(V)*** [35]**:**

A mixture of the benzoxazinone **IV** (1 g, 3.3 mmol) in formamide (15 ml) was heated under reflux for 4 h. Then, the reaction mixture was kept to cool at room temperature. The obtained solid product was collected by filtration, washed with water, dried at 120 °C and crystallized from ethanol.

Buff crystals, (yield 80 %), m.p. 320-322°C; IR (KBr, ν_{max}/cm^{-1}): 3325 (NH), 1670 (C=O amide), 1597, 1562 (C=C); ^{1}H NMR (DMSO-d_6)δ *ppm*: 7.59 (dd, *J*= 4.84, 4.84 Hz, 1H, Ar-H), 7.71 (d, *J*= 8.68 Hz, 1H, Ar-H), 8.00 (dd, *J*= 2.36, 2.36 Hz, 1H, Ar-H), 8.24 (d, *J*= 2.24 Hz, 1H, Ar-H), 8.50 – 8.47 (m, 1H, Ar-H), 8.77 (dd, *J*= 1.28, 1.32 Hz, 1H, Ar-H), 9.29 (d, *J*=1.96 Hz, 1H, Ar-H), 12.90 (s, 1H, D_2O exchangeable, -NH).

4.1.4. 6-Bromo-4-chloro-2-(pyridin-3-yl)quinazoline ***(VI)*** [36,37]**:**

A mixture of quinazolin-4-one **V** (0.5 g, 1.65 mmol) in $POCl_3$ (4 ml) was heated under reflux for 2.5 h. The reaction mixture was kept to cool at room temperature, poured dropwisely onto crushed ice-water with vigorous stirring and neutralized with 20% NaOH. The obtained solid product was filtered, washed with water, dried and crystallized from ethanol.

Olive green powder, (yield 85 %), m.p. 166-169°C; IR (KBr, ν_{max}/cm^{-1}): 3082 (CH aromatic), 1558, 1539 (C=C); ^{1}H NMR (DMSO-d_6)δ *ppm*: 7.64 (dd, *J*= 4.80, 4.80 Hz, 1H, Ar-H), 8.07 (d, *J*= 8.92 Hz, 1H, Ar-H), 8.25 (dd, *J*= 2.00, 2.04 Hz, 1H, Ar-H), 8.42 (d, *J*= 2.00 Hz, 1H, Ar-H), 8.72 - 8.78 (m, 2H, Ar-H), 9.56 (d, *J*=1.68 Hz, 1H, Ar-H).

4.1.5. General procedure for the preparation of compounds ***VIIa-c****:*

A mixture of equimolar amounts of 4-chloro derivative **VI** and the appropriate benzothiazole (10 mmol) was stirred under reflux in dry dimethylformamide (DMF) (10 ml) in presence of anhydrous potassium carbonate (K_2CO_3) (0.4 g, 3 mmol) for 15 h. The solid separated upon pouring the reaction mixture onto ice-water was filtered, washed with water, dried and crystallized from ethanol.

4.1.5.1. N-(6-bromo-2-(pyridin-3-yl)quinazolin-4-yl)benzo[d]thiazol-2-amine ***(VIIa)***

Dark brown powder, (yield 55%), m.p. 378-380°C; IR (KBr, ν_{max}/cm^{-1}): 3369 (NH), 1608 (NH bending), 1508 and 1435 (C=C); ^{1}H NMR (DMSO-d_6) δ *ppm*: 7.35 (t, *J*= 7.54 Hz, 1H, Ar-H), 7.50 (t, *J*= 7.56 Hz, 1H, Ar-H), 7.63 – 7.67 (m, 2H, Ar-H), 7.88 (d, *J*= 6.34 Hz, 2H, Ar-H), 8.77 (d, *J*= 3.76 Hz, 1H, Ar-H), 8.92 (d, *J*= 7.69 Hz, 1H, Ar-H), 8.56 - 8.67 (m, 2H, Ar-H), 8.97 (s, ½ H, D_2O exchangeable, -NH), 9.79 (s, 1H, Ar-H), 12.99 (s, ½ H, D_2O exchangeable, -NH) ; ^{13}C NMR (DMSO-d_6) δ *ppm*: 119.82, 122.59, 123.80, 124.18, 124.70, 127.08, 128.00, 130.43, 133.48, 136.12, 137.17, 138.76, 149.60, 150.07, 151.66, 158.16, 171.28; MS, *m/z*: 434 [M^+], 436 $[M+2]^+$; Anal. Calcd. % for $C_{20}H_{12}BrN_5S$ (434.32): C, 55.31; H, 2.79; N, 16.13; Found % C, 55.46; H, 2.84; N, 16.45.

4.1.5.2. N-(6-bromo-2-(pyridin-3-yl)quinazolin-4-yl)-6-ethoxybenzo[d] thiazol-2-amine ***(VIIb)***

Dark brown powder, (yield 56%), m.p. 383-385°C; IR (KBr, ν_{max}/cm^{-1}): 3394 (NH), 1604 (NH bending), 1523 and 1458 (C=C); ^{1}H NMR (DMSO-d_6) δ *ppm*: 1.38 (t, *J*= 6.92 Hz, 3H, $OCH_2C\underline{H_3}$), 4.12 (q, *J*= 6.86 Hz, 2H, $OC\underline{H_2}CH_3$), 7.07 (dd, *J*= 2.48, 2.40 Hz, 1H, Ar-H), 7.50 – 7.67 (m, 4H, Ar-H), 7.88 (d, *J*= 8.84, 1H, Ar-H), 8.06 (d, *J*= 8.92, 1H, Ar-H), 8.79 (t, *J*= 7.68, 1H, Ar-H), 8.93 (d, *J*= 8.00 Hz, 1H, Ar-H), 9.02 (s, 1H, D_2O exchangeable, -NH), 9.79 (d, *J*= 1.52, 1H, Ar-H); ^{13}C NMR (DMSO-d_6) δ *ppm*:15.19 ($OCH_2\underline{C}H_3$), 64.04 ($O\underline{C}H_2CH_3$), 116.17, 117.54, 120.14, 124.24, 127.24, 130.51, 133.83, 136.19, 137.23, 139.90, 150.11, 151.73, 155.85, 158.27, 171.62; MS, *m/z*: 478 [M^+], 480 $[M+2]^+$; Anal. Calcd. % for $C_{22}H_{16}BrN_5OS$ (478.37): C, 55.24; H, 3.37; N, 14.64; Found % C, 55.40; H, 3.49; N, 14.91.

4.1.5.3. N-(6-bromo-2-(pyridin-3-yl)quinazolin-4-yl)-6-nitrobenzo[d]thiazol-2-amine ***(VIIc)***

Red powder, (yield 63%), m.p. 378-380°C; IR (KBr, ν_{max}/cm^{-1}): 3373 (NH), 1608 (NH bending), 1508 and 1435 (C=C); ^{1}H NMR (DMSO-d_6) δ *ppm*: 7.56 – 7.64 (m, 2H, Ar-H), 7.72 (d, *J*= 8.76 Hz, 1H, Ar-H), 7.78 (dd, *J*= 2.28, 2.28 Hz, 1H, Ar-H), 8.15 (dd, *J*= 2.36, 2.4 Hz, 1H, Ar-H), 8.67 (s, 1H, D_2O exchangeable, -NH), 8.73 – 8.79 (m, 3H, Ar-H), 9.02 (d, *J*= 8.00 Hz, 1H, Ar-H), 9.84 (d, *J*= 1.32 Hz, 1H, Ar-H); ^{13}C NMR (DMSO-d_6) δ *ppm*: 117.84, 121.61, 122.65, 124.04, 127.91, 129.64, 134.41, 134.88, 135.39, 136.24, 140.28, 149.56, 150.27, 151.09, 157.57, 158.97, 161.62, 170.99; MS, *m/z*: 479 [M^+], 481 [M+2] $^+$; Anal. Calcd. % for $C_{20}H_{11}BrN_6O_2S$ (479.31): C, 50.12; H, 2.31; N, 17.53; Found % C, 50.31; H, 2.57; N, 17.75.

4.1.6. General procedure for the preparation of compounds ***(VIIIa-f)***

A mixture of equimolar amounts of 4-chloro derivative **VI** and the appropriate phenol (10 mmol) was stirred at room temperature in dry DMF (10 ml) in presence of anhydrous K_2CO_3 for 24 h. The solid separated upon pouring the reaction mixture onto ice-water was filtered, washed with water, dried and crystallized from ethanol.

4.1.6.1. 6-Bromo-4-phenoxy-2-(pyridin-3-yl)quinazoline ***(VIIIa)***

Grey powder, (yield 75%), m.p. 169-172°C; IR (KBr, ν_{max}/cm^{-1}): 3059 (CH aromatic str.), 1566 and 1550 (C=C); ^{1}H NMR (DMSO-d_6) *δ ppm*: 7.41 (t, *J*= 7.16 Hz, 1H, Ar-H), 7.51 (t, *J*= 8.38Hz, 3H, Ar-H), 7.57 - 7.61 (m, 2H, Ar-H), 8.01 (d, *J*= 8.88Hz, 1H, Ar-H), 8.19 (d, *J*= 8.68 Hz, 1H, Ar-H), 8.45 (d, *J*= 7.84 Hz, 1H, Ar-H), 8.53 (s, 1H, Ar-H), 8.68 (d, *J*= 3.88 Hz, 1H, Ar-H), 9.27 (s, 1H, Ar-H); ^{13}C NMR (DMSO-d_6) *δ ppm*: 116.45, 121.01, 122.45, 124.25, 126.25, 126.59, 130.18, 130.52, 132.61, 135.55, 138.53, 149.59, 150.95, 152.11, 152.43, 158.07, 166.18; MS, *m/z*: 378 [M^+], 380 [M+2]$^+$; Anal. Calcd. % for $C_{19}H_{12}BrN_3O$ (378.23): C, 51.02; H, 3.53; N, 17.50; Found % C, 51.30; H, 3.71; N, 17.69.

4.1.6.2. 6-Bromo-2-(pyridin-3-yl)-4-(p-tolyloxy)quinazoline ***(VIIIb):***

Grey powder, (yield 70%), m.p. 170-173°C; IR (KBr, ν_{max}/cm^{-1}): 2935 (CH aliphatic) 1550 and 1504 (C=C); ^{1}H NMR (DMSO-d_6) *δ ppm*: 2.42 (s, 3H, -CH_3), 7.30 – 7.42 (m, 4H, Ar-H), 7.52 (dd, *J*= 4.88, 4.80Hz, 1H, Ar-H), 8.01 (d, *J*= 8.84Hz, 1H, Ar-H), 8.19 (d, *J*= 8.88 Hz, 1H, Ar-H), 8.48 (d, *J*= 7.84 Hz, 1H, Ar-H), 8.52 (s, 1H, Ar-H), 8.67 (d, *J*= 4.48 Hz, 1H, Ar-H), 9.28 (s, 1H, Ar-H); ^{13}C NMR (DMSO-d_6) *δ ppm*: 21.03 ($\underline{C}H_3$), 115.47, 120.96, 122.09, 124.27, 126.25, 130.15, 130.50, 132.67, 135.58, 138.49, 149.61, 150.21, 152.12; MS, *m/z*: 392 [M^+], 394 [M+2] $^+$; Anal. Calcd. % for $C_{20}H_{14}BrN_3O$ (392.26): C, 54.76; H, 2.99; N, 15.96; Found % C, 54.97; H, 3.12; N, 16.14.

4.1.6.3. 6-Bromo-4-(4-fluorophenoxy)-2-(pyridin-3-yl)quinazoline ***(VIIIc)***

Grey powder, (yield 73%), m.p. 193-195°C; IR (KBr, ν_{max}/cm^{-1}): 3062 (CH aromatic), 1550 and 1504 (C=C); ^{1}H NMR (DMSO-d_6) *δ ppm*: 7.40 - 7.44 (m, 2H, Ar-H), 7.51 –

7.57 (m, 3H, Ar-H), 8.02 (d, *J*= 8.92 Hz, 1H, Ar-H), 8.20 (dd, *J*= 2.20, 2.20 Hz, 1H, Ar-H), 8.46 – 8.48 (m, 1H, Ar-H), 8.54 (d, *J*= 2.08 Hz, 1H, Ar-H), 8.68 (dd, *J*= 1.48, 1.44 Hz, 1H, Ar-H), 9.29 (d, *J*= 1.44 Hz, 1H, Ar-H); ^{13}C NMR (DMSO-d_6) δ *ppm*: 116.41, 116.67, 116.91, 121.04, 124.32, 124.41, 126.27, 130.53, 132.58, 135.60, 138.60, 149.58, 150.94, 152.16; MS, *m/z*: 396 [M$^+$], 398 [M+2]$^+$; Anal. Calcd. % for $C_{19}H_{11}BrFN_3O$ (396.22): C, 58.08; H, 3.71; N, 16.13; Found % C, 58.30; H, 3.88; N, 16.41.

4.1.6.4. 4-[{6-Bromo-2-(pyridin-3-yl)quinazolin-4-yl}oxy]benzaldehyde ***(VIIId)***

Grey powder, (yield 75%), m.p. 173-175°C; IR (KBr, νmax / cm-1): 2819 and 2792 (CH aldehydic), 1693(C=O), 1550 and 1489 (C=C); ^{1}H NMR (DMSO-d_6) δ *ppm*: 7.51 (dd, *J*= 4.8, 4.85Hz, 1H, Ar-H), 7.75 (d, *J*= 8.48Hz, 2H, Ar-H), 8.00 (d, *J*= 8.92 Hz, 1H, Ar-H), 8.13 (d, *J*= 8.48 Hz, 2H, Ar-H), 8.18 (dd, *J*= 2.16, 2.12 Hz, 1H, Ar-H), 8.44 (d, *J*= 8 Hz, 1H, Ar-H), 8.52 (d, *J*= 2.04 Hz, 1H, Ar-H), 8.66 (dd, *J*= 1.36, 1.32Hz, 1H, Ar-H), 9.26 (d, *J*= 1.44 Hz, 1H, Ar-H), 10.09 (s, 1H, CH aldehydic); ^{13}C NMR (DMSO-d_6) δ *ppm*: 116.21, 121.18, 123.24, 124.21, 126.14, 130.45, 131.71, 132.36, 134.42, 135.54, 138.63, 149.52, 150.96, 152.10, 156.94, 157.84, 165.54, 192.55 (C=O); MS, *m/z*: 406 [M$^+$], 408 [M+2]$^+$; Anal. Calcd. % for $C_{20}H_{12}BrN_3O_2$ (406.24): C, 59.42; H, 3.49; N, 17.32; Found % C, 59.76; H, 3.58; N, 17.56.

4.1.6.5. 6-Bromo-4-(4-nitrophenoxy)-2-(pyridin-3-yl)quinazoline ***(VIIIe)***

Grey powder, (yield 70%), m.p. 237-239°C; IR (KBr, ν_{max}/cm^{-1}): 3078 (CH aromatic), 1554 and 1519 (C=C); ^{1}H NMR (DMSO-d_6) δ *ppm*: 7.54 (dd, *J*= 4.96, 4.84 Hz, 1H, Ar-H), 7.84 (d, *J*= 9.04 Hz, 2H, Ar-H), 8.07 (d, *J*= 8.88 Hz, 1H, Ar-H), 8.25 (dd, *J*= 2.08, 2 Hz, 1H, Ar-H), 8.46 - 8.52 (m, 3H, Ar-H), 8.61 (d, *J*= 1.80 Hz, 1H, Ar-H), 8.7 (d, *J*= 3.48, 1H, Ar-H), 9.33 (s, 1H, Ar-H); ^{13}C NMR (DMSO-d_6) δ *ppm*: 116.25, 121.29, 123.74, 124.32, 125.95, 126.22, 130.51, 132.38, 135.71, 138.79, 145.54, 149.55, 151.07, 152.18, 157.27, 157.86; MS, *m/z*: 423 [M$^+$], 425 [M+2]$^+$; Anal. Calcd. % for $C_{19}H_{11}BrN_4O_3$ (423.23): C, 53.47; H, 2.92; N, 18.71; Found % C, 53.70; H, 3.06; N, 18.94.

4.1.6.6. N-[4-{(6-bromo-2-(pyridin-3-yl)quinazolin-4-yl)oxy}phenyl] acetamide ***(VIIIf)***

Grey powder, (yield 80%), m.p. 254-258°C; IR (KBr, ν_{max}/cm^{-1}): 3251(NH), 3066 (CH aromatic), 2951 (CH aliphatic), 1670 (C=O), 1620 (NH bending), 1566 and 1508 (C=C); ^{1}H NMR (DMSO-d_6) δ *ppm*: 2.10 (s, 3H,-CH_3), 7.40 (d, *J*= 8.84 Hz, 2H, Ar-H), 7.53 (dd,

J= 4.80, 4.84 Hz , 1H, Ar-H), 7.76 (d, J= 8.84 Hz, 2H, Ar-H), 8.01 (d, J= 8.92 Hz, 1H, Ar-H), 8.18 (dd, J= 2.12, 2.08 Hz, 1H, Ar-H), 8.48 (d, J= 8.04 Hz, 1H, Ar-H), 8.53 (d, J= 1.88 Hz, 1H, Ar-H), 8.68 (t, J= 2.34 Hz, 1H, Ar-H), 9.30 (s, 1H, Ar-H), 10.12 (s, 1H, D_2O exchangeable, -NH); ^{13}C NMR (DMSO-d_6) δ *ppm*: 24.48 ($\underline{C}H_3$), 120.30, 120.99, 122.59, 124.27, 126.24, 130.52, 132.65, 135.58, 137.66, 138.51, 147.47, 149.61, 152.11, 158.12, 168.85 (C=O); MS, *m/z*: 435 [M^+], 437 $[M+2]^+$; Anal. Calcd. % for $C_{21}H_{15}BrN_4O_2$ (435.28): C, 58.90; H, 4.33; N, 17.17; Found % C, 59.17; H, 4.54; N, 17.45.

*4.1.7. General procedure for the preparation of compounds **(IXa-d):***

A mixture of equimolar amounts of quinazolin-4-yl oxy benzaldehyde **VIIId** and the appropriate phenyl hydrazine derivative (1.23 mmol) was stirred under reflux in absolute ethanol (10 ml) in presence of glacial acetic acid (5 drops) for 9.5 - 24 h, whereas compound **IXb** and **IXc** were prepared by stirring at room temperature for 24 h. The obtained solid was filtered, washed with water and crystallized from ethanol.

*4.1.7.1. 6-Bromo-4-[4-{(2-phenylhydrazinylidene)methyl}phenoxy]-2-(pyridin-3-yl)quinazoline **(IXa)***

Off white powder, (yield 76%), m.p. 235-238°C; reaction time: 9.5 h; IR (KBr, ν_{max}/cm^{-1}): 3313 (NH), 1600 (NH bending), 1550 and 1481 (C=C); ^1H NMR (DMSO-d_6) δ *ppm*: 6.77 (t, J= 7.16 Hz, 1H, Ar-H), 7.12 (d, J= 7.96 Hz, 2H, Ar-H), 7.24 (t, J= 7.68 Hz, 2H, Ar-H), 7.53 (t, J= 6.66 Hz, 3H, Ar-H), 7.85 (d, J= 8.44 Hz, 2H, Ar-H), 7.97 (s, 1H, -C$\underline{H}$=N), 8.04 (d, J= 8.88 Hz, 1H, Ar-H), 8.21 (dd, J= 1.68, 1.72 Hz, 1H, Ar-H), 8.50 (d, J= 8 Hz, 1H, Ar-H), 8.57 (d, J= 1.48 Hz, 1H, Ar-H), 8.69 (d, J= 3.96 Hz, 1H, Ar-H), 9.33 (s, 1H, Ar-H), 10.43 (s, 1H, D_2O exchangeable, -NH); ^{13}C NMR (DMSO-d_6) δ *ppm*: 112.51, 116.47, 119.28, 121.05, 122.73, 124.30, 126.27, 127.18, 129.60, 130.54, 132.64, 134.22, 135.62, 136.05, 138.57 ($\underline{C}$H=N), 145.73, 149.62, 150.99, 152.01, 152.13, 158.11, 166.15; MS, *m/z*: 496 [M^+], 498 $[M+2]^+$; Anal. Calcd. % for $C_{26}H_{18}BrN_5O$ (496.37): C, 62.91; H, 3.66; N, 14.11; Found % C, 63.13; H, 3.58; N, 14.46.

*4.1.7.2. 6-Bromo-4-[4-{(2-(4-chlorophenyl)hydrazinylidene)methyl}phenoxy]-2-(pyridin-3-yl)quinazoline **(IXb)***

Yellow powder, (yield 70%), m.p. 232-235°C; reaction time: 24 h; IR (KBr, ν_{max}/cm^{-1}): 3221 (NH), 1604 (NH bending), 1562 and 1485 (C=C); ^{1}H NMR (DMSO-d_6) δ *ppm*: 7.11 (d, *J*= 8.68 Hz, 2H, Ar-H), 7.25 (d, *J*= 8.68 Hz, 2H, Ar-H), 7.53 (d, *J*= 8.48 Hz, 2H, Ar-H), 7.84 (d, *J*= 8.48 Hz, 3H, Ar-H), 7.98 (s, 1H, -CH=N), 8.04 (d, *J*= 8.92 Hz, 1H, Ar-H), 8.22 (dd, *J*= 1.72, 1.72 Hz, 1H, Ar-H), 8.57 (d, *J*= 1.52 Hz, 1H, Ar-H), 8.77 (d, *J*= 8.04 Hz, 1H, Ar-H), 8.85 (d, *J*= 4.64 Hz, 1H, Ar-H), 9.30 (s, 1H, Ar-H), 10.69 (s, 1H, D_2O exchangeable, -NH); ^{13}C NMR (DMSO-d_6) δ *ppm*: : 113.55, 116.04, 120.11, 121.72, 122.50, 123.21, 125.07, 127.37, 128.50, 129.25, 136.87, 138.08 (CH=N), 144.64, 145.06, 147.70, 150.73, 152.01, 156.32, 158.34, 161.44, 166.24 ;MS, *m/z*: 530 [M^{+}], 532 [M+2]$^{+}$; Anal. Calcd. % for $C_{26}H_{17}BrClN_5O$ (530.81): C, 58.83; H, 3.23; N, 13.19; Found % C, 58.64; H, 3.45; N, 13.42.

4.1.7.3. 6-Bromo-4-[4-{(2-(4-methoxyphenyl)hydrazinylidene)methyl} phenoxy]-2-(pyridin-3-yl)quinazoline ***(IXc)***

Violet powder, (yield 70%), m.p. 195-197°C; reaction time: 18 h; IR (KBr, ν_{max}/cm^{-1}): 3228 (NH), 1612 (NH bending), 1558 and 1504 (C=C); ^{1}H NMR (DMSO-d_6) δ *ppm*: 3.70 (s, 3H, -OCH$_3$), 6.85 (d, *J*= 8.84 Hz, 2H, Ar-H), 7.05 (d, *J*= 8.84 Hz, 2H, Ar-H), 7.50 (d, *J*= 8.52 Hz, 2H, Ar-H), 7.80 (d, *J*= 8.56 Hz, 3H, Ar-H), 7.91 (s, 1H, -CH=N), 8.04 (d, *J*= 8.96 Hz, 1H, Ar-H), 8.22 (dd, *J*= 2.04, 2.00 Hz, 1H, Ar-H), 8.57 (d, *J*= 1.84 Hz, 1H, Ar-H), 8.74 (d, *J*= 8.04 Hz, 1H, Ar-H), 8.83 (d, *J*= 4.6 Hz, 1H, Ar-H), 9.34 (s, 1H, Ar-H), 10.30 (s, 1H, D_2O exchangeable, -NH); ^{13}C NMR (DMSO-d_6) δ *ppm*: 55.73 (-OCH$_3$), 113.19, 115.08, 116.58, 120.08, 121.67, 123.16, 125.01, 126.29, 126.90, 127.35, 127.56, 128.47, 128.47, 134.54, 138.77, 139.74 (CH=N), 140.31, 150.67, 151.53, 153.12, 156.30, 157.90, 161.41, 166.19; MS, *m/z*: 526 [M^{+}], 528 [M+2]$^{+}$; Anal. Calcd. % for $C_{27}H_{20}BrN_5O_2$ (526.39): C, 61.61; H, 3.83; N, 13.30; Found % C, 61.89; H, 4.06 N, 13.46.

4.1.7.4. 4-[2-{4-((6-Bromo-2-(pyridin-3-yl)quinazolin-4-yl)oxy)benzylidene} hydrazinyl]benzenesulfonamide ***(IXd)***

Grey powder, (yield 50%), m.p. 289-292°C; reaction time: 18 h; IR (KBr, ν_{max}/cm^{-1}): 3421 and 3331 (NH$_2$), 3294 (NH), 1602 (NH bending), 1566 and 1485 (C=C), 1319 and 1141 (-SO$_2$); ^{1}H NMR (DMSO-d_6) δ *ppm*: 7.09 (s, 2H, D_2O exchangeable, -NH$_2$), 7.20

(d, *J*= 8.48 Hz, 2H, Ar-H), 7.45 (d, *J*= 7.96 Hz, 1H, Ar-H), 7.55 (d, *J*= 8.16 Hz, 2H, Ar-H), 7.69 (d, *J*= 8.52 Hz, 2H, Ar-H), 7.89 (d, *J*= 8.36 Hz, 2H, Ar-H), 8.02 (d, = 8.88 Hz, 1H, Ar-H), 8.05 (s, 1H, CH=N), 8.20 (d, *J*= 8.44 Hz, 1H, Ar-H), 8.51 (d, *J*= 7.92 Hz, 1H, Ar-H), 8.56 (s, 1H, Ar-H), 8.69 (d, *J*= 3.96 Hz, 1H, Ar-H), 9.32 (s, 1H, Ar-H), 10.90 (s, 1H, D_2O exchangeable, -NH); ^{13}C NMR (DMSO-d_6) δ *ppm*: 111.73, 116.42, 121.09, 122.79, 124.39, 126.24, 127.69, 127.96, 130.51, 132.70, 133.63, 134.01, 135.86, 138.59 (CH=N), 148.22, 149.35, 150.94, 151.85, 152.48, 157.95, 166.06; MS, *m/z*: 575 [M^+], 577 [M+2] $^+$; Anal. Calcd. % for $C_{26}H_{19}BrN_6O_3S$ (575.44): C, 54.27; H, 3.33; N, 14.60; Found % C, 54.60; H, 3.48; N, 14.86.

4.1.8. 6-Bromo-4-hydrazinyl-2-(pyridin-3-yl)quinazoline ***(X):***

A mixture of 4-chloroquinazoline derivative **VI** (0.5 g, 1.5 mmol) and hydrazine hydrate (99%) (3 ml, 96.3 mmol) was stirred under reflux for 8.5 h. The obtained solid was filtered off, dried and crystallized from ethanol/chloroform mixture.

Buff powder, (yield 80%), m.p. 353-355°C; IR (KBr, ν_{max}/cm^{-1}): 3300 and 3294 (NH_2), 3209 (NH), 1639 and 1589 (NH bending), 1566 and 1527(C=C); ^{1}H NMR (DMSO-d_6) δ *ppm*: 5.02 (s, 2H, D_2O exchangeable, -NH_2), 7.53 (dd, *J*= 4.84, 4.84 Hz, 1H, Ar-H), 7.71 (d, *J*= 8.80 Hz, 1H, Ar-H), 7.90 (d, *J*= 8.72 Hz, 1H, Ar-H), 8.51 (s, 1H, Ar-H), 8.70 (d, *J*= 4.48 Hz, 1H, Ar-H), 8.82 (d, *J*= 7.80 Hz, 1H, Ar-H), 9.69 (s, 1H, Ar-H), 9.86 (s, 1H, D_2O exchangeable, -NH); ^{13}C NMR (DMSO-d_6) δ *ppm*: 114.81, 118.30, 123.86, 125.45, 130.38, 133.94, 135.81, 136.19, 148.64, 149.99, 151.41, 158.70, 159.19; MS, *m/z*: 316 [M^+], 318 [M+2] $^+$; Anal. Calcd. % for $C_{13}H_{10}BrN_5$ (316.16): C, 49.39; H, 3.19; N, 22.15; Found % C, 49.70; H, 3.42; N, 22.37.

4.1.9. General procedure for the preparation of compounds ***(XIa-c)***

An equimolar amount of 4-hydrazinyl derivative **X** and appropriate acid anhydride (1.6 mmol) in least amount of glacial acetic acid (10 ml) was stirred under reflux for 6 – 13 h. Compound **Xlb** was prepared by refluxing in acetic anhydride (10 ml) for 4.5 h. The obtained solid was filtered off after cooling to room temperature, washed with water, dried and crystallized from ethanol to afford the corresponding **XIa-c**.

4.1.9.1. 1-[(6-bromo-2-(pyridin-3-yl)quinazolin-4-yl)amino]pyrrolidine-2,5-dione ***(XIa)***

White powder, (yield 65%), m.p. 337-340°C; reaction time: 6 h; IR (KBr, ν_{max}/cm^{-1}): 3348 (-NH), 1728 and 1712 (2 C=O), 1593 (NH bending), 1566 and 1527 (C=C); ^{1}H NMR (DMSO-d_6) δ *ppm*: 2.99 – 3.10 (m, 4H, -C<u>H</u>$_2$-C<u>H</u>$_2$-), 7.55 (dd, *J*= 4.84, 4.84 Hz, 1H, Ar-H), 7.91 (d, *J*= 8.92 Hz, 1H, Ar-H), 8.10 (dd, *J*= 1.60, 1.60 Hz, 1H, Ar-H), 8.58 (d, *J*= 7.96 Hz, 1H, Ar-H), 8.71 (d, *J*= 2.24 Hz, 2H, Ar-H), 9.44 (s, 1H, Ar-H), 11.10 (s, 1H, D_2O exchangeable, -NH); ^{13}C NMR (DMSO-d_6) δ *ppm*: 27.02 (-CH_2-CH_2-), 113.89, 119.86, 124.30, 125.80, 130.93, 133.06, 135.78, 137.69, 149.43, 149.50, 151.83, 158.08, 158.20, 175.04 (2 <u>C</u>=O); MS, *m/z*: 398 [M^+], 400 [M+2] $^+$; Anal. Calcd. % for $C_{17}H_{12}BrN_5O_2$ (398.22): C, 51.27; H, 3.04; N, 17.59; Found % C, 51.49; H, 3.27; N, 17.80.

4.1.9.2. N-acetyl-N'-(6-bromo-2-(pyridin-3-yl)quinazolin-4-yl)acetohydrazide ***(XIb)***

White powder, (yield 65%), m.p. 337-340°C; reaction time: 4.5 h; IR (KBr, ν_{max}/cm^{-1}): 3448 (-NH), 1716 and 1714 (2 C=O), 1593 (NH bending), 1562 and 1535(C=C); ^{1}H NMR (DMSO-d_6) δ *ppm*: 2.45 (s, 6H, 2 -CH_3), 7.59 – 7.66 (m, 1H, Ar-H), 7.90 (d, *J*= 8.88 Hz, 1H, Ar-H), 8.09 (t, *J*= 8.84 Hz, 1H, Ar-H), 8.60 – 8.77 (m, 3H, Ar-H), 9.45 (d, *J*= 6.08 Hz, 1H, Ar-H), 11.10 (s, 1H, D_2O exchangeable, -NH); ^{13}C NMR (DMSO-d_6) δ *ppm*: 25.27, 25.53 (2 -<u>C</u>H_3), 114.25, 119.57, 121.42, 124.44, 125.84, 129.04, 130.86, 132.54, 133.41, 135.87, 137.60, 149.07, 151.25, 152.07, 157.92, 158.08, 159.44, 172.49 (2 <u>C</u>=O); MS, *m/z*: 400 [M^+], 402 [M+2] $^+$; Anal. Calcd. % for $C_{17}H_{14}BrN_5O_2$ (400.24): C, 51.02; H, 3.53; N, 17.50; Found % C, 51.34; H, 3.68; N, 17.78.

4.1.9.3. 2-[(6-bromo-2-(pyridin-3-yl)quinazolin-4-yl]amino)isoindoline-1,3-dione ***(XIc)***

White powder, (yield 65%), m.p. 351-353°C; reaction time: 13 h; IR (KBr, ν_{max}/cm^{-1}): 3356 (-NH), 1732 and 1716 (2 C=O), 1612 (NH bending), 1566 and 1527(C=C); ^{1}H NMR (DMSO-d_6) δ *ppm*: 7.37 (dd, *J*= 4.84, 4.88 Hz, 1H, Ar-H), 7.92 (d, *J*= 8.92 Hz, 1H, Ar-H), 8.05 – 8.14 (m, 5H, Ar-H), 8.34 (d, *J*= 8 Hz, 1H, Ar-H), 8.56 (d, *J*= 3.96 Hz, 1H, Ar-H), 8.77 (s, 1H, Ar-H), 9.03 (s, 1H, Ar-H), 11.4 (s, 1H, D_2O exchangeable, -NH); ^{13}C NMR (DMSO-d_6) δ *ppm*: 113.88, 120.05, 124.06, 124.51, 125.85, 130.08, 130.92, 132.85, 135.24, 136.11, 137.82, 149.13, 149.52, 151.75, 157.95, 158.51, 166.42 (2 <u>C</u>=O);

MS, *m/z*: 446 [M$^+$], 448 [M+2] $^+$; Anal. Calcd. % for $C_{21}H_{12}BrN_5O_2$ (446.26): C, 56.52; H, 2.71; N, 15.69; Found % C, 56.52; H, 2.71; N, 15.69.

*4.1.10. General procedure for the preparation of compounds **(XIIa-c):***

A mixture of 4-hydrazinyl derivative **X** (0.5 g, 1.6 mmol) and appropriate acid chloride (1.7 mmol) in presence of triethylamine (0.22 ml, 1.6 mmol) was stirred at room temperature in dry methylene chloride (10 ml) for 10 - 72 h. The obtained solid was filtered, washed with water/methanol, dried and crystallized from methanol/DMF to afford the corresponding **XIIa-c**.

*4.1.10.1. N'-(6-bromo-2-(pyridin-3-yl)quinazolin-4-yl)-4-cyanobenzohydrazide **(XIIa)***

Dark yellow powder, (yield 70%), m.p. 316-319°C; reaction time: 34 h; IR (KBr, ν_{max}/cm^{-1}): 3290 and 3248 (2 -NH), 2225 (CN), 1643 (C=O), 1600 (NH bending), 1539 and 1458 (C=C); ^{1}H NMR (DMSO-*d$_6$*) *δ ppm*: 7.52 (dd, *J*= 4.96, 4.96 Hz, 1H, Ar-H), 7.85 (d, *J*= 8.96 Hz, 1H, Ar-H), 8.06 (t, *J*= 6.84 Hz, 1H, Ar-H), 8.11 (d, *J*= 8.24 Hz, 2H, Ar-H), 8.18 (d, *J*= 8.20 Hz, 2H, Ar-H), 8.62 – 8.70 (m, 3H, Ar-H), 9.44 (s, 1H, Ar-H), 10.71 (s, 1H, D_2O exchangeable, -NH), 11.13 (s, 1H, D_2O exchangeable, -NH); ^{13}C NMR (DMSO-*d$_6$*) *δ ppm*: 114.83, 115.03, 118.60 (CN), 119.30, 125.64, 128.80, 130.17, 135.60, 136.33, 137.24, 149.93, 151.73, 158.69, 165.04 (C=O) MS, *m/z*: 445 [M$^+$], 447 [M+2] $^+$; Anal. Calcd. % for $C_{21}H_{13}BrN_6O$ (445.28): C, 56.65; H, 2.94; N, 18.87; Found % C, 56.72; H, 3.12; N, 19.15.

*4.1.10.2. N'-(6-bromo-2-(pyridin-3-yl)quinazolin-4-yl)-4-methoxybenzo hydrazide **(XIIb)***

Dark yellow powder, (yield 70%), m.p. 316-319°C; reaction time: 10 h; IR (KBr, ν_{max}/cm^{-1}): 3329 and 3255 (2 -NH), 2947 (-CH_3), 1658 (C=O), 1608 (NH bending), 1519 and 1496 (C=C); ^{1}H NMR (DMSO-*d$_6$*) *δ ppm*: 3.88 (s, 3H, -OCH_3), 7.13 (d, *J*= 8.56 Hz, 2H, Ar-H), 7.48 (dd, *J*= 5.08, 5.08 Hz, 1H, Ar-H), 7.85 (d, *J*= 8.88 Hz, 1H, Ar-H), 8.03 (d, *J*= 8.28 Hz, 3H, Ar-H), 8.60-8.65 (m, 2H, Ar-H), 8.71 (s, 1H, Ar-H), 9.44 (s, 1H, Ar-H), 10.54 (s, 1H, D_2O exchangeable, -NH), 10.68 (s, 1H, D_2O exchangeable, -NH); ^{13}C NMR (DMSO-*d$_6$*) *δ ppm*: 55.91 (-OCH_3),114.33, 114.72, 119.20, 124.04, 125.75, 130.73, 133.59, 135.91, 137.03, 149.62, 151.56, 158.53, 166.58 (C=O); MS, *m/z*: 450 [M$^+$], 452

[M+2] $^{+}$; Anal. Calcd. % for $C_{21}H_{16}BrN_5O_2$ (450.30): C, 56.01; H, 3.58; N, 15.55; Found % C, 55.89; H, 3.74; N, 15.81.

4.1.10.3. N'-(6-bromo-2-(pyridin-3-yl)quinazolin-4-yl)-4-chlorobenzohydrazide ***(XIIc)***

Yellow powder, (yield 65%), m.p. 299-302°C; reaction time: 72 h; IR (KBr, ν_{max}/cm^{-1}): 3290 and 3248 (2 -NH), 1643 (C=O), 1600 (NH bending), 1523 and 1485 (C=C); ^{1}H NMR (DMSO-d_6) δ *ppm*: 7.50 (dd, *J*= 4.76, 5.00 Hz, 1H, Ar-H), 7.69 (d, *J*= 8.28 Hz, 2H, Ar-H), 7.85 (d, *J*= 8.32 Hz, 1H, Ar-H), 8.05 (d, *J*= 8.16 Hz, 3H, Ar-H), 8.62 (d, *J*= 8.28 Hz, 1H, Ar-H), 8.65 (d, *J*= 3.88 Hz, 1H, Ar-H), 8.70 (s, 1H, Ar-H), 9.44 (s, 1H, Ar-H), 10.62 (s, 1H, D_2O exchangeable, -NH), 10.93 (s, 1H, D_2O exchangeable, -NH); ^{13}C NMR (DMSO-d_6) δ *ppm*: 119.28, 124.11, 125.76, 129.36, 129.87, 131.94, 135.60, 137.09, 137.38, 149.54, 151.60; MS, *m/z*: 454 [M^+], 456 [M+2] $^{+}$; Anal. Calcd. % for $C_{20}H_{13}BrClN_5O$ (454.71): C, 52.83; H, 2.88; N, 15.40; Found % C, 53.11; H, 3.04; N, 15.6.

General procedure for the preparation of compounds ***(XIIIa-d)*** [38–44]

4.1.11. General procedure for the preparation of compounds ***(XIVa-i.):***

A mixture of equimolar amount of 4-hydrazinyl derivative **X** and appropriate aldehyde (1.6 mmol) was stirred under reflux in absolute ethanol (10 ml) for 7 – 18 h. The obtained solid was filtered off, washed with absolute ethanol and crystallized from ethanol to afford the corresponding **XIVa-i**.

4.1.11.1. 4-(2-Benzylidenehydrazinyl)-6-bromo-2-(pyridin-3-yl)quinazoline ***(XIVa)***

Dark yellow powder, (yield 77%), m.p. 273–275 °C; reaction time: 15 h; IR (KBr, ν_{max}/cm^{-1}): 3394 (-NH), 1608 (NH bending), 1577 (-C=N), 1546 and 1485 (C=C); ^{1}H NMR (DMSO-d_6) δ *ppm*: 7.50 – 7.60 (m, 5H, Ar-H), 7.84 (d, *J*= 8.56 Hz, 3H, Ar-H), 8.02 (d, *J*= 8.88 Hz, 1H, Ar-H), 8.52 (s, 1H, -N=C<u>H</u>), 8.73 – 8.79 (m, 2H, Ar-H), 9.66 (s, 1H, Ar-H), 11.99 (s, 1H, D_2O exchangeable, -NH); ^{13}C NMR (DMSO-d_6) δ *ppm*: 114.60, 124.13, 127.48, 129.50, 130.59, 130.70, 133.70, 134.81, 135.72, 136.82, 149.78 (-N=<u>C</u>H), 151.61; MS, *m/z*: 404 [M^+], 406 [M+2] $^{+}$; Anal. Calcd. % for $C_{20}H_{14}BrN_5$ (404.27): C, 59.42; H, 3.49; N, 17.32; Found % C, 59.65; H, 3.70; N, 17.53.

4.1.11.2. 6-Bromo-4-[{3-phenylallylidene}hydrazinyl]-2-(pyridin-3-yl)quinazoline ***(XIVb)***

Dark yellow powder, (yield 61%), m.p. 227–230 °C; reaction time: 7 h; IR (KBr, ν_{max}/ cm^{-1}): 3421 (-NH), 1620 (NH bending), 1573 (-C=N), 1523 and 1481 (C=C); ^{1}H NMR (DMSO-d_6) δ *ppm*: 7.12 – 7.25 (m, 2H, Ar-H), 7.36 – 7.45 (m, 4H, Ar-H, -C<u>H</u>=C<u>H</u>-), 7.57 (dd, *J*= 4.92, 4.88 Hz, 1H, Ar-H), 7.71 (d, *J*= 7.44Hz, 2H, Ar-H), 7.82 (d, *J*= 8.88 Hz, 1H, Ar-H), 8.00 (d, *J*= 7.44 Hz, 1H, Ar-H), 8.34 (d, *J*= 8.36 Hz, 1H, -N=C<u>H</u>), 8.72 (d, *J*= 4.48 Hz, 1H, Ar-H), 8.76 (d, *J*= 7.80 Hz, 1H, Ar-H), 9.63 (s, 1H, Ar-H), 11.81 (s, 1H, D_2O exchangeable, -NH); ^{13}C NMR (DMSO-d_6) δ *ppm*:114.57, 118.90, 124.02, 125.94, 127.69, 129.32, 129.36, 130.61, 133.73, 135.75, 136.44, 136.81, 139.60, 149.82 (-N=<u>C</u>H), 151.54, 158.74; MS, *m/z*: 430 [M^+], 432 [M+2] $^+$; Anal. Calcd. % for $C_{22}H_{16}BrN_5$ (430.31): C, 66.41; H, 3.98; N, 13.83; Found % C, 66.74; H, 4.12; N, 14.07.

4.1.11.3. 6-Bromo-4-(2-(4-methoxybenzylidene)hydrazinyl)-2-(pyridin-3-yl) quinazoline ***(XIVc)***

Yellow powder, (yield 73%), m.p. 269–271 °C; reaction time: 15.5 h; IR (KBr, ν_{max}/cm^{-1}): 3448 (-NH), 1612 (NH bending), 1581 (-C=N), 1508 and 1485 (C=C); ^{1}H NMR (DMSO-d_6) δ *ppm*: 3.85 (s, 3H, -OC<u>H</u>$_3$), 7.10 (d, *J*= 8.44 Hz, 2H, Ar-H), 7.59 (dd, *J*= 4.76, 4.80 Hz, 1H, Ar-H), 7.78 (s, 1H, Ar-H), 7.82 (d, *J*= 9.12 Hz, 2H, Ar-H), 8.00 (d, *J*= 8.68 Hz, 1H, Ar-H), 8.46 (s, 1H, -N=C<u>H</u>), 8.72 (d, *J*= 4.32 Hz, 2H, Ar-H), 8.78 (d, *J*= 7.00 Hz, 1H, Ar-H), 9.65 (s, 1H, Ar-H), 11.84 (s, 1H, D_2O exchangeable, -NH); ^{13}C NMR (DMSO-d_6) δ *ppm*: 55.84 (-O<u>C</u>H$_3$), 115.04, 123.01, 124.10, 129.12, 130.65, 135.71, 136.73, 143.50, 147.90 (-N=<u>C</u>H), 150.20, 151.59, 161.39 ; MS, *m/z*: 434 [M^+], 436 [M+2] $^+$; Anal. Calcd. % for $C_{21}H_{16}BrN_5O$ (434.30): C, 58.08; H, 3.71; N, 16.13; Found % C, 58.31; H, 3.89; N, 16.40.

4.1.11.4. 6-Bromo-4-(2-(4-chlorobenzylidene)hydrazinyl)-2-(pyridin-3-yl) quinazoline ***(XIVd)***

Yellow powder, (yield 89%), m.p. 290–293 °C; reaction time: 18 h; IR (KBr, ν_{max}/cm^{-1}): 3421 (-NH), 1608 (NH bending), 1577 (-C=N), 1546 and 1485 (C=C); ^{1}H NMR (DMSO-d_6) δ *ppm*: 7.57 (s, 1H, Ar-H), 7.60 (d, *J*= 8.40 Hz, 2H, Ar-H), 7.85 (dd, *J*= 9.08, 8.52 Hz, 3H, Ar-H), 8.02 (d, *J*= 8.72 Hz, 1H, Ar-H), 8.50 (s, 1H, -N=C<u>H</u>), 8.73 – 8.80 (m, 2H, Ar-H), 8.91 (d, *J*= 6.20 Hz, 1H, Ar-H), 9.66 (s, 1H, Ar-H), 12.01 (s, 1H, D_2O exchangeable, -NH); ^{13}C NMR (DMSO-d_6) *δ ppm*: 114.51, 118.98, 124.08, 129.05, 129.55, 130.66, 133.75, 134.94, 135.73, 136.80, 149.77 (-N=C̲H), 151.56; MS, *m/z*: 438 [M^+], 440 $[M+2]^+$; Anal. Calcd. % for $C_{20}H_{13}BrClN_5$ (438.71): C, 54.76; H, 2.99; N, 15.96; Found % C, 54.94; H, 3.13; N, 16.21.

4.1.11.5. 6-Bromo-4-(2-(4-nitrobenzylidene)hydrazinyl)-2-(pyridin-3-yl)quinazoline ***(XIVe)***

Dark yellow powder, (yield 81%), m.p. 322-325 °C; reaction time: 7.5 h; IR (KBr, ν_{max}/cm^{-1}): 3444 (-NH), 1608 (NH bending), 1570 (-C=N), 1516 and 1481 (C=C); ^{1}H NMR (DMSO-d_6) *δ ppm*: 7.58 (s, 1H, Ar-H), 7.85 (d, *J* = 8.60 Hz, 1H, Ar-H), 8.02 (d, *J*= 8.60 Hz, 1H, Ar-H), 8.08 (d, *J*= 7.24 Hz, 2H, Ar-H), 8.36 (d, *J*= 7.96 Hz, 2H, Ar-H), 8.58 (s, 1H, -N=CH̲), 8.74 – 8.80 (m, 2H, Ar-H), 8.92 (d, *J*= 5.72 Hz, 1H, Ar-H), 9.66 (s, 1H, Ar-H), 12.21 (s, 1H, D_2O exchangeable, -NH); ^{13}C NMR (DMSO-d_6) *δ ppm*: 118.69, 120.19, 124.71, 131.36, 136.03, 138.70, 140.70, 143.36, 145.86, 149.70 (-N=C̲H), 152.03, 154.37, 160.37; MS, *m/z*: 449 [M^+], 451 $[M+2]^+$; Anal. Calcd. % for $C_{20}H_{13}BrN_6O_2$ (449.27): C, 53.47; H, 2.92; N, 18.71; Found % C, 53.75; H, 3.09; N, 19.04.

4.1.11.6. 6-Bromo-4-[2-{4-(piperidin-1-yl)benzylidene}hydrazinyl]-2-(pyridin-3-yl) quinazoline ***(XIVf)***

Buff powder, (yield 60%), m.p. 257–260 °C; reaction time: 10.5 h; IR (KBr, ν_{max}/cm^{-1}): 3421 (-NH), 1608 (NH bending), 1573 (-C=N), 1512 and 1473 (C=C); ^{1}H NMR (DMSO-d_6) *δ ppm*: 1.60 (s, 10H, piperidinyl Hs), 7.04 (d, *J*= 8.56 Hz, 2H, Ar-H), 7.56 – 7.66 (m, 4H, Ar-H), 7.80 (d, *J*= 8.88 Hz, 1H, Ar-H), 7.98 (d, *J*= 8.84 Hz, 1H, Ar-H), 8.37 (s, 1H, -N=CH̲), 8.72 (d, *J*= 4.00 Hz, 1H, Ar-H), 8.77 (d, *J*= 6.72 Hz, 1H, Ar-H), 9.64 (s, 1H, Ar-H), 11.71 (s, 1H, D_2O exchangeable, -NH); ^{13}C NMR (DMSO-d_6) *δ ppm*: 24.42 (-CH_2-C̲H_2-CH_2-), 25.42 (-C̲H_2-CH_2-C̲H_2-), 48.84 (-C̲H_2-N-C̲H_2-), 115.17, 124.06, 128.84, 130.55, 135.68, 136.58, 149.77 (-N=C̲H), 151.50, 152.86; MS, *m/z*: 487 [M^+], 489 $[M+2]^+$; Anal. Calcd. % for $C_{25}H_{23}BrN_6$ (487.41): C, 61.61; H, 4.76; N, 17.24; Found % C, 61.87; H, 4.89; N, 17.52.

4.1.11.7. 4-[4-{(2-(6-Bromo-2-(pyridin-3-yl)quinazolin-4-yl)hydrazinylidene) methyl}phenyl]morpholine ***(XIVg)***

Yellow powder, (yield 75%), m.p. 274–277 °C; reaction time: 10.5 h; IR (KBr, ν_{max}/cm^{-1}): 3448 (-NH), 1608 (NH bending), 1573 (-C=N), 1516 and 1473 (C=C); ^{1}H NMR (DMSO-d_6) δ *ppm*: 3.25 (t, *J*= 4.04 Hz, 4H, -C$\underline{H_2}$-N-C$\underline{H_2}$-), 3.77 (t, *J*= 3.84 Hz, 4H, C$\underline{H_2}$-O-C$\underline{H_2}$), 7.08 (d, *J*= 8.6 Hz, 2H, Ar-H), 7.58 (dd, *J*= 4.88, 4.84 Hz, 1H, Ar-H), 7.70 (d, *J*= 6.88 Hz, 2H, Ar-H), 7.81 (d, *J*= 8.88 Hz, 1H, Ar-H), 8.00 (d, *J*= 8.8 Hz, 1H, Ar-H), 8.41 (s, 1H, -N=C$\underline{H}$), 8.72 (d, *J*= 4.52, 2H, Ar-H), 8.77 (d, *J*= 6.60 Hz, 1H, Ar-H), 9.65 (s, 1H, Ar-H), 11.79 (s, 1H, D_2O exchangeable, -NH); ^{13}C NMR (DMSO-d_6) δ *ppm*: 47.90 ($\underline{C}H_2$-N-$\underline{C}H_2$), 66.42 ($\underline{C}H_2$-O-$\underline{C}H_2$), 114.96, 124.05, 128.71, 130.56, 135.68, 136.59, 149.77 (-N=$\underline{C}$H), 151.50, 152.69; MS, *m/z*: 489 [M$^+$], 491 [M+2]$^+$; Anal. Calcd. % for $C_{24}H_{21}BrN_6O$ (489.38): C, 58.90; H, 4.33; N, 17.17; Found % C, 59.12; H, 4.56; N, 17.41.

4.1.11.8. 6-Bromo-4-[2-{4-(4-methylpiperazin-1-yl)benzylidene}hydrazinyl]-2-(pyridin-3-yl)quinazoline ***(XIVh)***

Dark yellow powder, (yield 85%), m.p. 257–259 °C; reaction time: 17.5 h; IR (KBr, ν_{max}/cm^{-1}): 3421 (-NH), 1604 (NH bending), 1573 (-C=N), 1512 and 1477 (C=C); ^{1}H NMR (DMSO-d_6) δ *ppm*: 2.23 (s, 3H, -C$\underline{H_3}$), 2.46 (t, *J*= 5.1 Hz, 4H, piperazine H_3, H_5), 3.28 (t, *J*= 5.1 Hz, 4H, piperazine H_2, H_6), 7.06 (d, *J*= 8.64 Hz, 2H, Ar-H), 7.58 (dd, *J*= 4.88, 4.88 Hz, 1H, Ar-H), 7.60 – 7.70 (m, 2H, Ar-H), 7.79 (d, *J*= 8.68 Hz, 1H, Ar-H), 7.97 (d, *J*= 8.64 Hz, 1H, Ar-H), 8.4 (s, 1H, -N=C$\underline{H}$), 8.72 – 8.76 (m, 3H, Ar-H), 9.63 (s, 1H, Ar-H), 11.73 (s, 1H, D_2O exchangeable, -NH); ^{13}C NMR (DMSO-d_6) δ *ppm*: 46.19 (-$\underline{C}H_3$), 47.52 (piperazine C_3, C_5), 54.85 (piperazine C_2, C_6), 115.09, 124.05, 128.75, 130.54, 133.86, 135.69, 136.56, 149.76 (-N=$\underline{C}$H), 151.50, 152.58; MS, *m/z*: 502 [M$^+$], 504 [M+2]$^+$; Anal. Calcd. % for $C_{25}H_{24}BrN_7$ (502.42): C, 59.77; H, 4.82; N, 19.52; Found % C, 60.03; H, 4.98; N, 19.74.

4.1.11.9. 6-Bromo-4-[2-{4-(4-phenylpiperazin-1-yl)benzylidene}hydrazinyl]-2-(pyridin-3-yl)quinazoline ***(XIVi)***

Dark yellow powder, (yield 78%), m.p. 273–275 °C; reaction time: 17.5 h; IR (KBr, ν_{max}/cm^{-1}): 3421 (-NH), 1600 (NH bending), 1570 (-C=N), 1512 and 1473 (C=C); ^{1}H NMR (DMSO-d_6) δ *ppm*: 3.30 (s, 8H, piperazine Hs), 6.83 (t, *J* = 7.16 Hz, 1H, Ar-H), 7.01 (d, *J*= 8.12 Hz, 2H, Ar-H), 7.13 (d, *J*= 8.60 Hz, 2H, Ar-H), 7.26 (t, *J*= 7.70 Hz, 2H, Ar-H), 7.60 (dd, *J*= 4.96, 4.72 Hz, 1H, Ar-H), 7.72 (s, 1H, Ar-H), 7.81 (d, *J*= 8.36 Hz, 2H, Ar-H), 8.01 (d, *J*= 8.76 Hz, 1H, Ar-H), 8.43 (s, 1H, -N=C<u>H</u>), 8.73 – 8.78 (m, 3H, Ar-H), 9.65 (s, 1H, Ar-H), 11.78 (s, 1H, D_2O exchangeable, -NH); ^{13}C NMR (DMSO-d_6) δ *ppm*: 47.69 (piperazine C_3, C_5), 48.60 (piperazine C_2, C_6), 115.13, 116.12, 119.67, 124.13, 128.80, 129.46, 130.69, 135.80, 136.57, 149.65, 151.26, 151.42, 152.42, 158.70; MS, *m/z*: 564 [M$^+$], 566 [M+2]$^+$; Anal. Calcd. % for $C_{30}H_{26}BrN_7$ (564.49): C, 63.83; H, 4.64; N, 17.37; Found % C, 64.09; H, 4.88; N, 17.59.

4.2. Biological evaluation

Biological evaluation was performed in the laboratory of the Egyptian company for the production of vaccines, sera, and drugs (VACSERA, Giza, Egypt).

4.2.1. EGFR-TK inhibitory assay

Cells were seeded into each well in a 96 well plate and incubated overnight at 37 °C, and under 5% CO_2. The tested compounds were dissolved into serum free cell culture medium, and then the cells were treated with 4 concentrations (2, 10, 50 and 250 nM) of tested compounds. Each well was washed by pipetting 200 μL of the prepared 1X wash buffer A. The plate was washed 4 times with 1X wash buffer A, and then the plate was tapped upside down to remove all of wash buffer. 200 μL of prepared 1X blocking buffer was added and was incubated for 1 h at 37 °C to remove all of excess wash buffer. 50 μL of 1X Anti-Phospho-EGFR (activated) was added to corresponding wells and was incubated for 2 hours at room temperature while shaking. The plate was washed 4 times with 200 μL 1X wash buffer B. 50 μL of 1X Anti-Mouse IgG (HRP-conjugated secondary antibody) was added and was incubated at room temperature for 1 h. The plate was washed 4 times with 200 μL 1X wash buffer B. 100 μL of TMB was added to each well and incubated for 30 min with shaking at room temperature in the dark. 50 μL of stop solution was added to each well and read at 450 nm, measure OD immediately.

4.2.2. In vitro cytotoxic activity

Experiments were run on four human tumor cell lines, **MCF-7** (breast carcinoma cell line) and **A549, PC9** and **HC827** (lung carcinoma cell lines). The cell lines were obtained from the American type collection. For best results, cells in the log phase of growth were employed and each test included a blank containing complete medium without cells. reconstituted MTT were added in an amount equal to 10% of the culture medium volume. Cultures were returned to incubator for 2-4 hours depending on cell type and maximum cell density. After the incubation period, cultures were removed from the incubator and the resulting formazan crystals were dissolved by adding an amount of MTT Solubilization Solution [M-8910] equal to the original culture medium volume the mixed gently. Absorbance was measured spectrophotometrically at a wavelength of 570 nm.

4.2.3. Cell Cycle Analysis

Breast **MCF-7** cells obtained from American Type Culture Collection were seeded with a density of 1×10^6 cells/well in RPMI 1640 containing 10% fetal bovine serum at 37°C for 24 h. Cells were treated with 0.01 μM of the tested compound **VIIa** per well in a 6-well plate for 24 h before the enzyme assay. Cells were fixed with 70% ethanol for 30 min at 4°C. Then, cells were centrifuged (1200 rpm for 5 min), the supernatant layer was discarded and the pellet washed with PBS and stained the cells with propidium iodide staining buffer (PI 200 mg), 0.1% (v/v) Triton X-100, 2 mg DNAse-free RNAse A (Sigma) in PBS (10 ml) for 15 min at ambient temperature in absence of light. Later, samples were analyzed for propidium iodide-DNA fluorescence from 10,000 events flow cytometry, using BD-FACS Calibur flow cytometry reader.

4.2.4. Apoptotic Assay

Briefly, cells were incubated and treated to induce apoptosis as discussed in cell cycle analysis. The cells were collected by trypsinisation and washed twice with ice-cold PBS, then resuspended in 500 μl of 1X Binding Buffer. 5 μl of Annexin V-FITC and 5 μl of propidium iodide were added to cells and incubated at room temperature for 15 min in the dark. After incubation, cells were quantified by analyzing Annexin V-FITC binding by flow cytometry at wavelength 488 nm using BD-FACS Calibur flow cytometry reader.

4.3. Molecular Modeling Study

4.3.1. Molecular docking study:

All the molecular modeling studies were accomplished using Molecular Operating Environment (MOE, 2010.10) software. All minimizations were achieved with MOE until an RMSD gradient of 0.1 kcal·mol^{-1}Å^{-1} with MMFF94x force field and the partial charges were automatically calculated. The X-ray crystallographic structure (PDB ID: 1XKK) of EGFR enzyme co-crystallized with **Lapatinib** as inhibitor (IC_{50}= 10.2 nM) was downloaded from the protein data bank [45,46]. All ligands and water molecules that are not involved in binding were removed. One conserved water molecule involved in the co-crystalized ligand binding to the EGFR binding site was kept **Figure 4**. The protein structure was prepared for docking study using *Protonate 3D* protocol in MOE with default options. The co-crystalized ligand (**Lapatinib**) was used to define the active site for the docking algorithm. Triangle Matcher placement method was used to perform docking, whereas, Affinity dG and London dG scoring functions were used for initial docking pose and refined docking pose scoring, respectively. Docking protocol was first validated by self-docking of the co-crystallized ligand (**Lapatinib**) in the vicinity of the enzyme active site giving energy score (S) = −15.11 kcal/mol and RMSD of 1.63 Å as shown in **Figure 5**. The validated docking protocol was then used to study the ligand-target interactions in the active site for the most potent newly synthesized compounds **VIIa**,**c**, **VIIIf**, **IXb**, **XIc**, **XIIb** and **XIVe** to predict their binding mode to rationalize their promising activity.

4.3.2. Physicochemical, ADME and pharmacokinetic properties prediction:

The free Swiss ADME web tool available from the Swiss Institute of Bioinformatics (SIB) was used for the calculation of the physicochemical descriptors as well as to predict the ADME parameters, pharmacokinetic properties, drug-like nature and medicinal chemistry friendliness of the most potent newly synthesized compounds **VIIa**,**c** , **VIIIf**, **IXb**, **XIc**, **XIIb** and **XIVe** [47–50]. The compounds' structures were converted to SMILES notations, then submitted to the online server for calculation.

References

[1] G.S. Hassan, Synthesis and antitumor activity of certain new thiazolo[2,3-b]quinazoline and thiazolo[3,2-a]pyrimidine analogs, Med. Chem. Res. 23 (2014)

388–401.

[2] V.T. DeVita, E. Chu, A history of cancer chemotherapy, Cancer Res. 68 (2008) 8643–8653.

[3] V.V. Padma, An overview of targeted cancer therapy, BioMedicine. 5 (2015) 19. doi:10.7603/s40681-015-0019-4.

[4] F. Broekman, E. Giovannetti, G.J. Peters, Tyrosine kinase inhibitors: Multi- targeted or single-targeted?, World J. Clin. Oncol. 2 (2011) 80–93.

[5] M. Topcul, I. Cetin, Endpoint of cancer treatment: targeted therapies., Asian Pac. J. Cancer Prev. 15 (2014) 4395–403.

[6] R.S.M. Ismail, S.M. Abou-Seri, W.M. Eldehna, N.S.M. Ismail, S.M. Elgazwi, H.A. Ghabbour, M.S. Ahmed, F.T. Halaweish, D.A. Abou El Ella, Novel series of 6-(2-substitutedacetamido)-4-anilinoquinazolines as EGFR-ERK signal transduction inhibitors in MCF-7 breast cancer cells, Eur. J. Med. Chem. 155 (2018) 782–796.

[7] M.N. Noolvi, H.M. Patel, Synthesis, method optimization, anticancer activity of 2,3,7-trisubstituted quinazoline derivatives and targeting EGFR-tyrosine kinase by rational approach., Arab. J. Chem. 6 (2013) 35–48.

[8] R. Guda, R. Korra, S. Balaji, R. Palabindela, R. Eerla, Design, synthesis and biological evaluation of 8-substituted-6- hydrazonoindolo[2,1-b]quinazolin-12(6H)-one scaffolds as potential cytotoxic agents: IDO-1 targeting molecular docking studies, Bioorg. Med. Chem. Lett. 27 (2017) 4741–4748.

[9] R. Guda, S. Narsimha, R. Babu, S. Muthadi, H. Lingabathula, Novel substituted hydrazono indolo[2,1-b]quinazoline-6,12-dione analogues as cytostatic agents: Synthesis, crystal structure, biological evaluation and molecular docking studies, Bioorg. Med. Chem. Lett. 26 (2016) 5517–5523. doi:10.1016/j.bmcl.2016.10.006.

[10] W.H. Ward, P.N. Cook, A.M. Slater, D.H. Davies, G.A. Holdgate, L.R. Green, Epidermal growth factor receptor tyrosine kinase. Investigation of catalytic mechanism, structure-based searching and discovery of a potent inhibitor., Biochem. Pharmacol. 48 (1994) 659–66

[11] A.J. Bridges, Chemical inhibitors of protein kinases., Chem. Rev. 101 (2001) 2541–72.

[12] M. Mphahlele, M. Mmonwa, A. Aro, L. McGaw, Y. Choong, Synthesis, biological evaluation and molecular docking of novel indole-aminoquinazoline hybrids for anticancer properties, Int. J. Mol. Sci. 19 (2018) 1–17.

[13] A.M. Al-Obaid, S.G. Abdel-Hamide, H.A. El-Kashef, A.A.-M. Abdel-Aziz, A.S. El-Azab, H.A. Al-Khamees, H.I. El-Subbagh, Substituted quinazolines, part 3. Synthesis, in vitro antitumor activity and molecular modeling study of certain 2-thieno-4(3H)-quinazolinone analogs, Eur. J. Med. Chem. 44 (2009) 2379–2391.

[14] G. da Cunha Santos, F.A. Shepherd, M.S. Tsao, EGFR Mutations and Lung Cancer, Annu. Rev. Pathol. Mech. Dis. 6 (2011) 49–69.

[15] N. Xu, W. Fang, L. Mu, Y. Tang, L. Gao, S. Ren, D. Cao, L. Zhou, A. Zhang, D. Liu, C. Zhou, K.K. Wong, L. Yu, L. Zhang, L. Chen, Overexpression of wildtype EGFR is tumorigenic and denotes a therapeutic target in non-small cell lung cancer, Oncotarget. 7 (2016) 3884–3896.

[16] J.M. Gee, J.F. Robertson, E. Gutteridge, I.O. Elis, S.E. Pinder, M. Rubini, R.I. Nicholson, Epidermal growth factor receptor/HER2/insulin-like growth factor receptor signalling and oestrogen receptor activity in clinical breast cancer, in: Endocr. Relat. Cancer, 2005: pp. S99–S111.

[17] G.D. Lewis, J.A. Lofgren, A.E. McMurtrey, A. Nuijens, B.M. Fendly, K.D. Bauer, M.X. Sliwkowski, Growth regulation of human breast and ovarian tumor cells by heregulin: Evidence for the requirement of ErbB2 as a critical component in mediating heregulin responsiveness., Cancer Res. 56 (1996) 1457–65.

[18] R. Mass, The role of HER-2 expression in predicting response to therapy in breast

cancer, Semin. Oncol. 27 (2000) 46–52.

[19] R.I. Nicholson, R.A. McClelland, P. Finlay, C.L. Eaton, W.J. Gullick, A.R. Dixon, J.F. Robertson, I.O. Ellis, R.W. Blamey, Relationship between EGF-R, c-erbB-2 protein expression and Ki67 immunostaining in breast cancer and hormone sensitivity., Eur. J. Cancer. 29A (1993) 1018–23.

[20] M. Moerkens, Y. Zhang, L. Wester, B. van de Water, J.H. Meerman, Epidermal growth factor receptor signalling in human breast cancer cells operates parallel to estrogen receptor α signalling and results in tamoxifen insensitive proliferation, BMC Cancer. 14 (2014) 283.

[21] K. Subik, J.F. Lee, L. Baxter, T. Strzepek, D. Costello, P. Crowley, L. Xing, M.C. Hung, T. Bonfiglio, D.G. Hicks, P. Tang, The expression patterns of ER, PR, HER2, CK5/6, EGFR, KI-67 and AR by immunohistochemical analysis in breast cancer cell lines, Breast Cancer Basic Clin. Res. 4 (2010) 35–41.

[22] H. Takeuchi, M. Baba, S. Shigeta, An application of tetrazolium (MTT) colorimetric assay for the screening of anti-herpes simplex virus compounds., J. Virol. Methods. 33 (1991) 61–71.

[23] M. Jaimes, M. Inokuma, C. McIntyre, D. Mittar, Detection of apoptosis using the BD Annexin V FITC assay on the BD FACSVerse™ system, BD Biosci. (2011) 1–12.

[24] W. Gorczyca, Cytometric analyses to distinguish death processes, Endocr. Relat. Cancer. 6 (1999) 17–19.

[25] C.A. Lipinski, F. Lombardo, B.W. Dominy, P.J. Feeney, Experimental and computational approaches to estimate solubility and permeability in drug discovery and development settings., Adv. Drug Deliv. Rev. 46 (2001) 3–26.

[26] A.K. Ghose, V.N. Viswanadhan, J.J. Wendoloski, A knowledge-based approach in designing combinatorial or medicinal chemistry libraries for drug discovery. 1. A qualitative and quantitative characterization of known drug databases., J. Comb. Chem. 1 (1999) 55–68.

[27] D.F. Veber, S.R. Johnson, H.-Y. Cheng, B.R. Smith, K.W. Ward, K.D. Kopple, Molecular properties that influence the oral bioavailability of drug candidates., J. Med. Chem. 45 (2002) 2615–23

[28] W.J. Egan, K.M. Merz, J.J. Baldwin, Prediction of drug absorption using multivariate statistics., J. Med. Chem. 43 (2000) 3867–77

[29] I. Muegge, S.L. Heald, D. Brittelli, Simple selection criteria for drug-like chemical matter., J. Med. Chem. 44 (2001) 1841–1846.

[30] T. Cheng, Y. Zhao, X. Li, F. Lin, Y. Xu, X. Zhang, Y. Li, R. Wang, L. Lai, Computation of octanol/water partition coefficients by guiding an additive model with knowledge, J. Chem. Inf. Model. 47 (2007) 2140–2148.

[31] R.R. Yadav, S.K. Guru, P. Joshi, G. Mahajan, M.J. Mintoo, V. Kumar, S.S. Bharate, D.M. Mondhe, R.A. Vishwakarma, S. Bhushan, S.B. Bharate, 6-Aryl substituted 4-(4-cyanomethyl)phenylamino quinazolines as a new class of isoform- selective PI3K-alpha inhibitors, Eur. J. Med. Chem. 122 (2016) 731–743

[32] X.D. Ma, N. Qiu, B. Yang, Q.J. He, Y.Z. Hu, Novel quinoline-derived mTOR inhibitors with remarkable enzymatic and cellular activities: Design, synthesis and biological evaluation, Medchemcomm. 7 (2016) 297–310.

[33] R. Article, M. Rangasamy, K.G. Parthiban, Synthesis and H1-antihistaminic activity of some 3-[(N,N-Dialkylamino)alkyl]-6-halo-2- thio-4(3H)- Quinazolinones., J. Pharm. Res. 3 (2010) 2628–2630.

[34] P.C. Sharma, S. Jain, Synthesis and in-vitro antibacterial activity of some novel N-nicotinoyl-1-ethyl-6-fluoro-1,4-dihydro-7-piperazin-1-yl-4-oxoquinoline-3-carboxylates, Acta Pol. Pharm. 65 (2008) 551–556.

[35] H. Suzuki, Masaki; Kondo, Kazumi; Kurimura, Muneaki; Valluru, Krishna Reddy; Takahashi, Akira; Kuroda, Takeshi; Fukushima, Tae; Miyamura, Shin Takahashi, Quinazoline derivatives as striatal-enriched tyrosine phosphatase modulators and their preparation and use as as therapeutic compounds, WO 2011/082337 Al, 2011.

[36] G. Pamukcu, Rifat; Piazza, Method for inhibiting neoplastic cells and related conditions by exposure to 4-aminoquinazoline derivatives, US 2002/00225968 A1,

2002.

[37] S.J. Lee, Y. Konishi, O. T. Macina, K. Kondo, D. T. Yu, 4-Aminoquinazoline derivatives, US005439895A, 1995.

[38] S. Lieber, F. Scheer, W. Meissner, S. Naruhn, T. Adhikary, S. Müller-Brüsselbach, W.E. Diederich, R. Müller, (Z)-2-(2-bromophenyl)-3-{[4-(1-methyl-piperazine)amino] phenyl}acrylonitrile (DG172): An orally bioavailable PPARβ/δ-selective ligand with inverse agonistic properties, J. Med. Chem. 55 (2012) 2858–2868.

[39] P.G. Mandhane, R.S. Joshi, D.R. Nagargoje, A. V. Chate, C.H. Gill, Ultrasonic promoted synthesis and antibacterial screening of some novel piperidine incorporated α-aminophosphonates, Phosphorus, Sulfur Silicon Relat. Elem. 186 (2011) 149–158.

[40] R.S. Joshi, P.G. Mandhane, S.D. Diwakar, S.K. Dabhade, C.H. Gill, Synthesis, analgesic and anti-inflammatory activities of some novel pyrazolines derivatives, Bioorganic Med. Chem. Lett. 20 (2010) 3721–3725.

[41] M. Mečiarová, Š. Toma, P. Magdolen, Ultrasound effect on the aromatic nucleophilic substitution reactions on some haloarenes, Ultrason. Sonochem. 10 (2003) 265–270.

[42] D. Kumar, K.K. Raj, M. Bailey, T. Alling, T. Parish, D.S. Rawat, Antimycobacterial activity evaluation, time-kill kinetic and 3D-QSAR study of C-(3-aminomethyl-cyclohexyl)-methylamine derivatives, Bioorganic Med. Chem. Lett. 23 (2013) 1365–1369.

[43] B.-Y. Li, H.-P; Guo, Can-Cheng; Ruan, Jianming; Huang, Synthesis, characterization and anticancer activity of piperazine substituted porphyrins, Chinese J. Org. Chem. 24 (2004) 783–787.

[44] Z.-Q. Liang, C.-X. Wang, J.-X. Yang, H.-W. Gao, Y.-P. Tian, X.-T. Tao, M.-H.

Jiang, A highly selective colorimetric chemosensor for detecting the respective amounts of iron(ii) and iron(iii) ions in water, New J. Chem. 31 (2007) 906.

[45] E.R. Wood, A.T. Truesdale, O.B. McDonald, D. Yuan, A. Hassell, S.H. Dickerson, B. Ellis, C. Pennisi, E. Horne, K. Lackey, K.J. Alligood, D.W. Rusnak, T.M. Gilmer, L. Shewchuk, A unique structure for epidermal growth factor receptor bound to GW572016 (Lapatinib): relationships among protein conformation, inhibitor off-rate, and receptor activity in tumor cells., Cancer Res. 64 (2004) 6652–6659.

[46] https://www.rcsb.org/structure/1XKK.

[47] A. Daina, V. Zoete, A BOILED-Egg to predict gastrointestinal absorption and brain penetration of small molecules, ChemMedChem. 11 (2016) 1117–1121.

[48] SwissADME, http://www.swissadme.ch/index.php#4.

[49] A. Daina, O. Michielin, V. Zoete, iLOGP: A simple, robust, and efficient description of n -octanol/water partition coefficient for drug design using the GBSA approach, J. Chem. Inf. Model. 54 (2014) 3284–3301.

[50] A. Daina, O. Michielin, V. Zoete, SwissADME: a free web tool to evaluate pharmacokinetics, drug-likeness and medicinal chemistry friendliness of small molecules, Sci. Rep. 7 (2017) 42717.

Design and Synthesis of some new 2,4,6-trisubstituted quinazoline EGFR inhibitors as targeted anticancer agents

Highlights

- The synthesis of 6-bromo-2-(pyridin-3-yl)-4-substituted quinazolines.
- The target compounds were evaluated as EGFR inhibitors compared to Gefitinib.
- The most active compounds were screened for their cytotoxicity
- Compound **VIIa** was subjected to cell cycle analysis and apoptotic assay.
- A molecular modeling study was achieved.

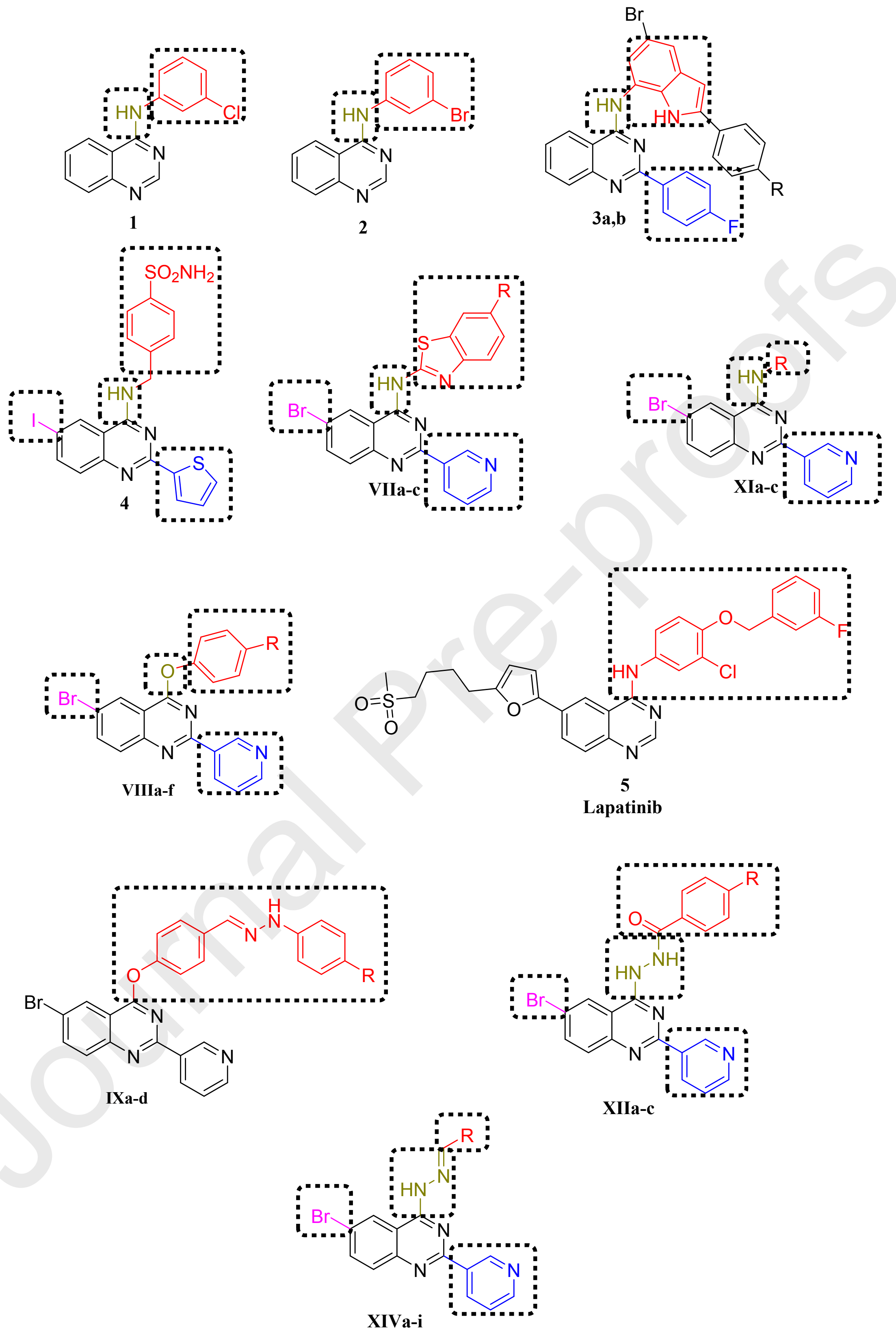

Fig. 1: Reported quinazoline anticancer agents, and the scaffold of the target compounds

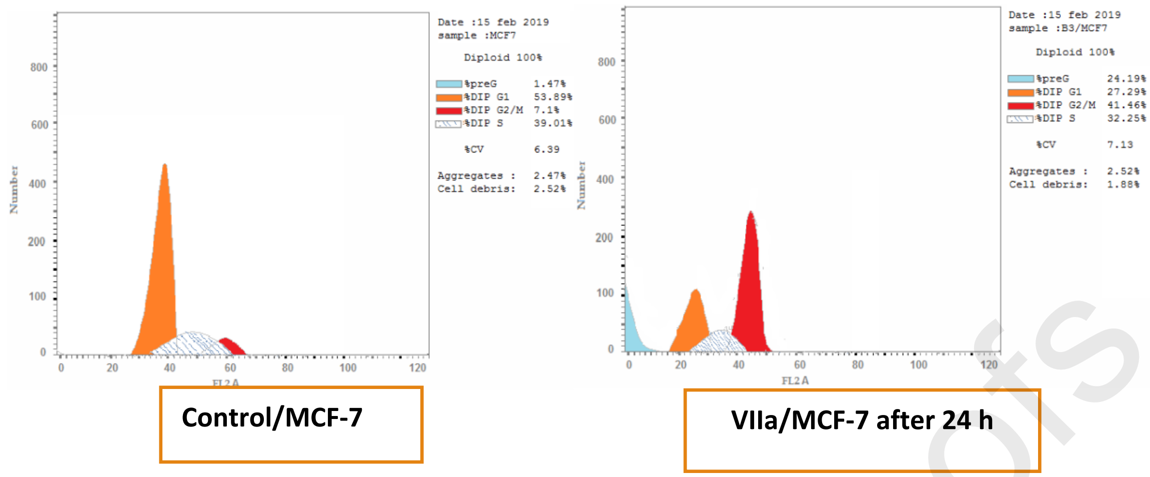

Fig. 2. Effect of compound **VIIa** on the cell cycle of **MCF-7** cells after 24 h.

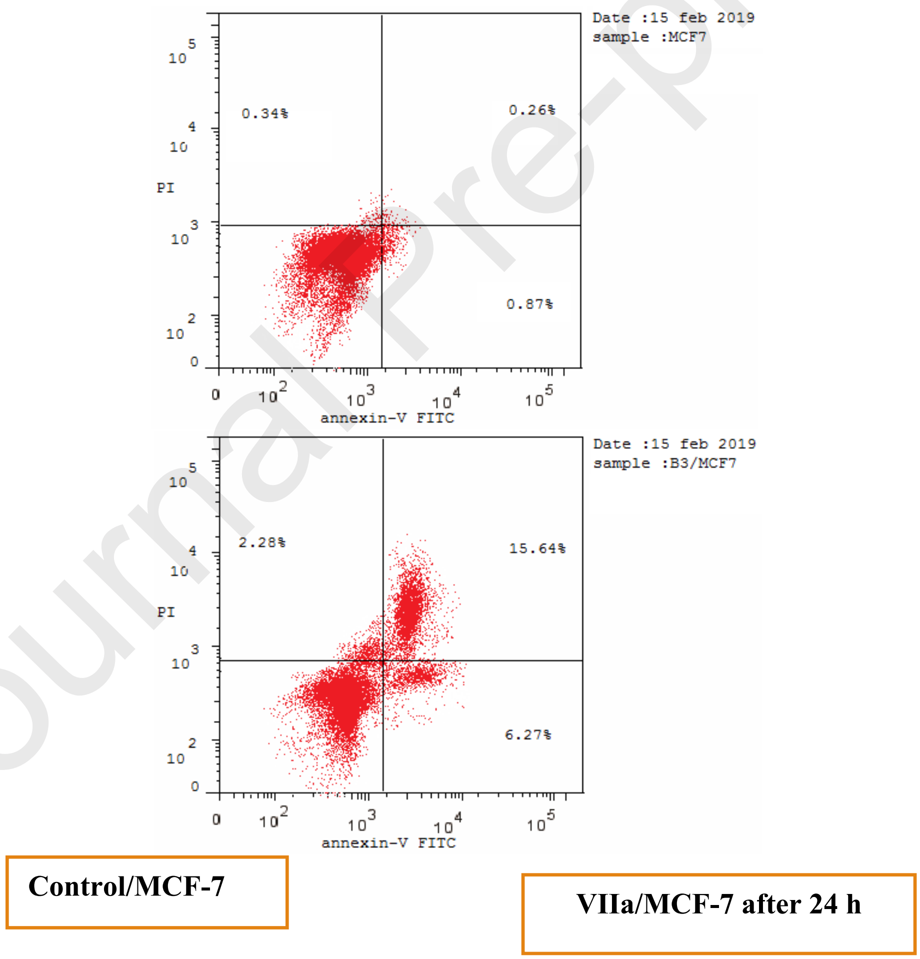

Fig. 3. Effect of compound **VIIa** on apoptosis induction of **MCF-7** cells after 24h.

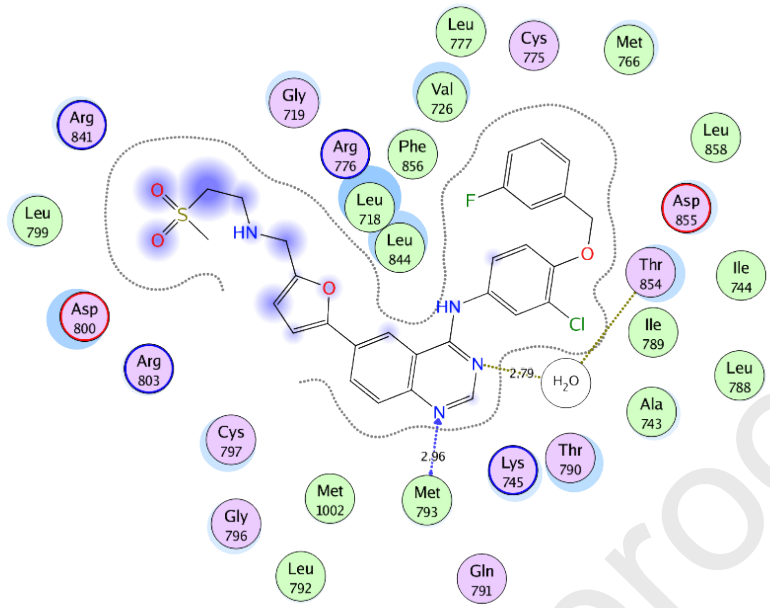

Fig. 4. 2D interaction diagram showing **Lapatinib** docking pose interactions with the key amino acids in the EGFR binding site.

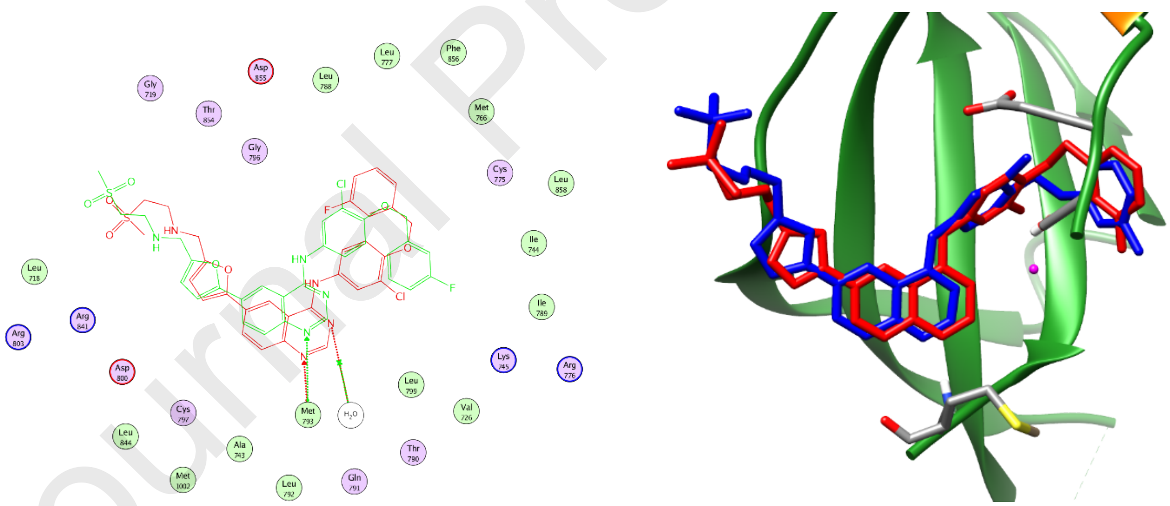

(a) **(b)**

Fig. 5. 2D diagram **(a)** and 3D representation **(b)** of the superimposition of the co-crystallized (red) and the docking pose (blue) of **Lapatinib** in the EGFR binding site with RMSD of 1.63Å. (ligand hydrogen atoms were removed for clarity)

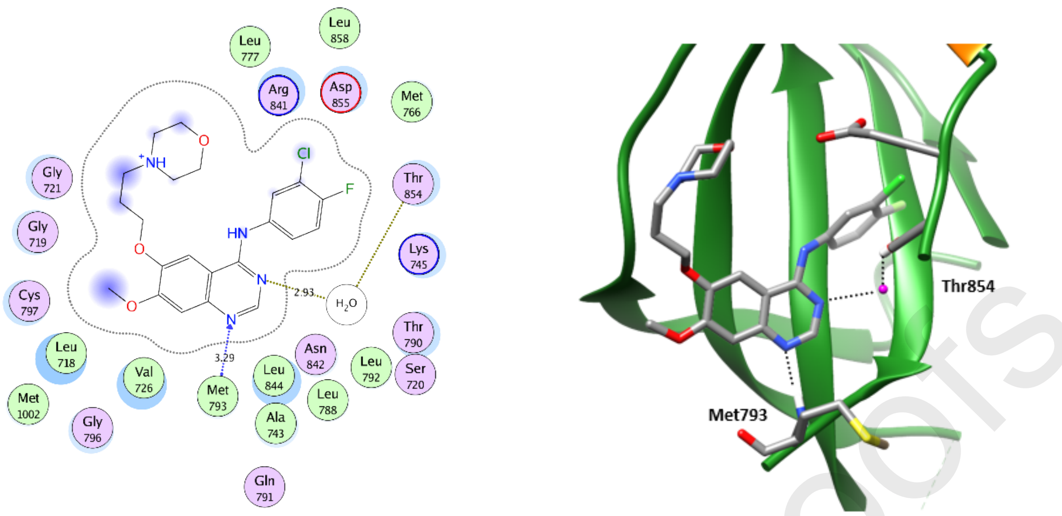

(a) **(b)**

Fig. 6. 2D diagram **(a)** and 3D representation **(b)** of **Gefitinib** in the EGFR binding site.

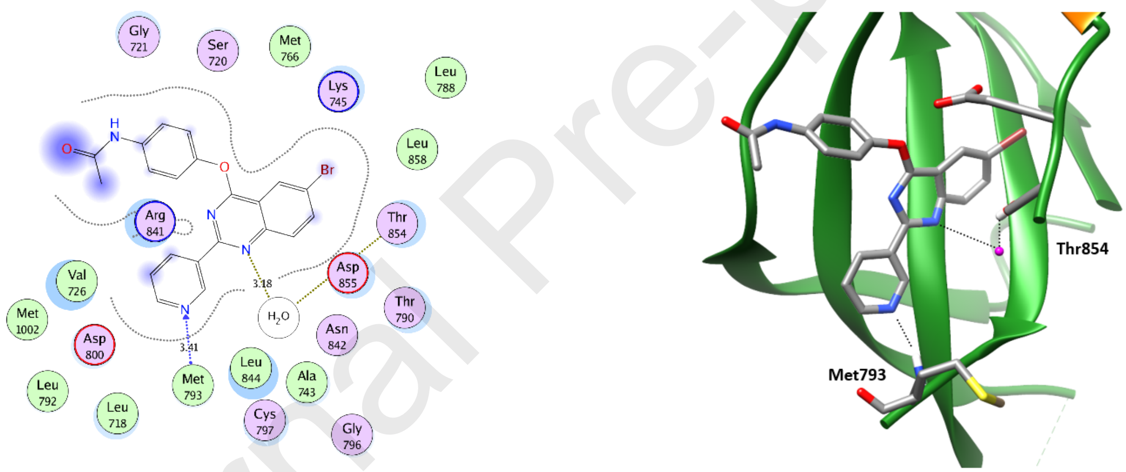

(a) **(b)**

Fig. 7. 2D diagram **(a)** and 3D representation **(b)** of compound **VIIIf** in the EGFR binding site.

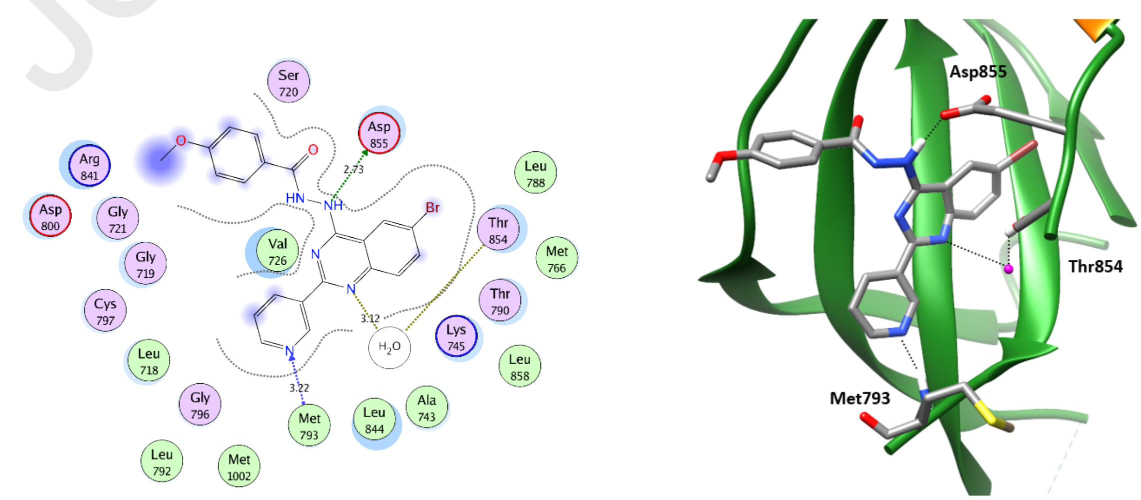

(a) (b)

Fig. 8. 2D diagram **(a)** and 3D representation **(b)** of compound **XIIb** in the EGFR binding site

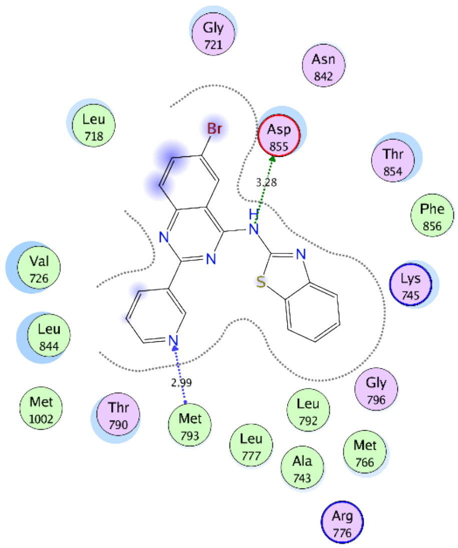

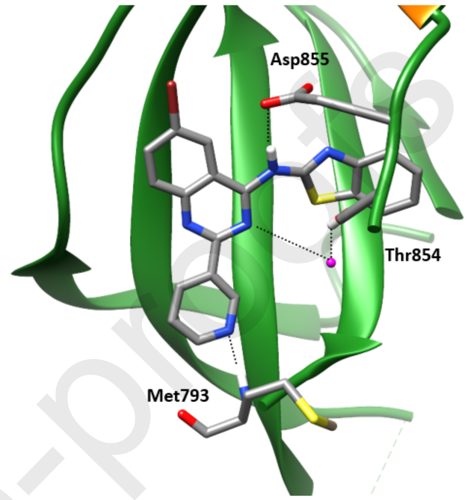

(a) (b)

Fig. 9. 2D diagram **(a)** and 3D representation **(b)** of compound **VIIa** in the EGFR binding site.

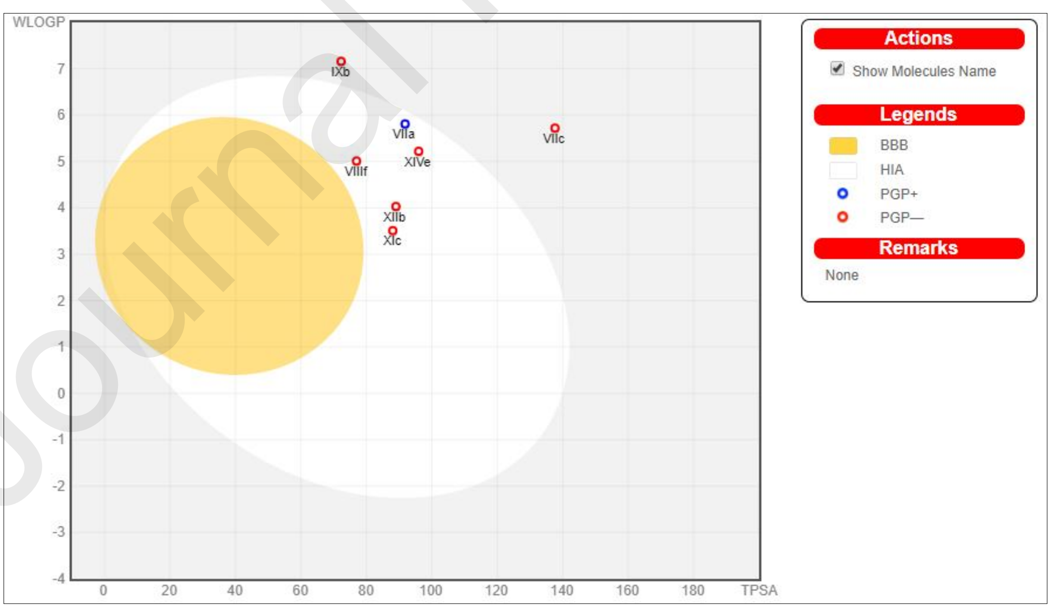

Fig. 10. Predicted Boiled-Egg plot from SwissADME online web tool for compounds **VIIa**,**c**, **VIIIf**, **IXb**, **XIc**, **XIIb** and **XIVe**.

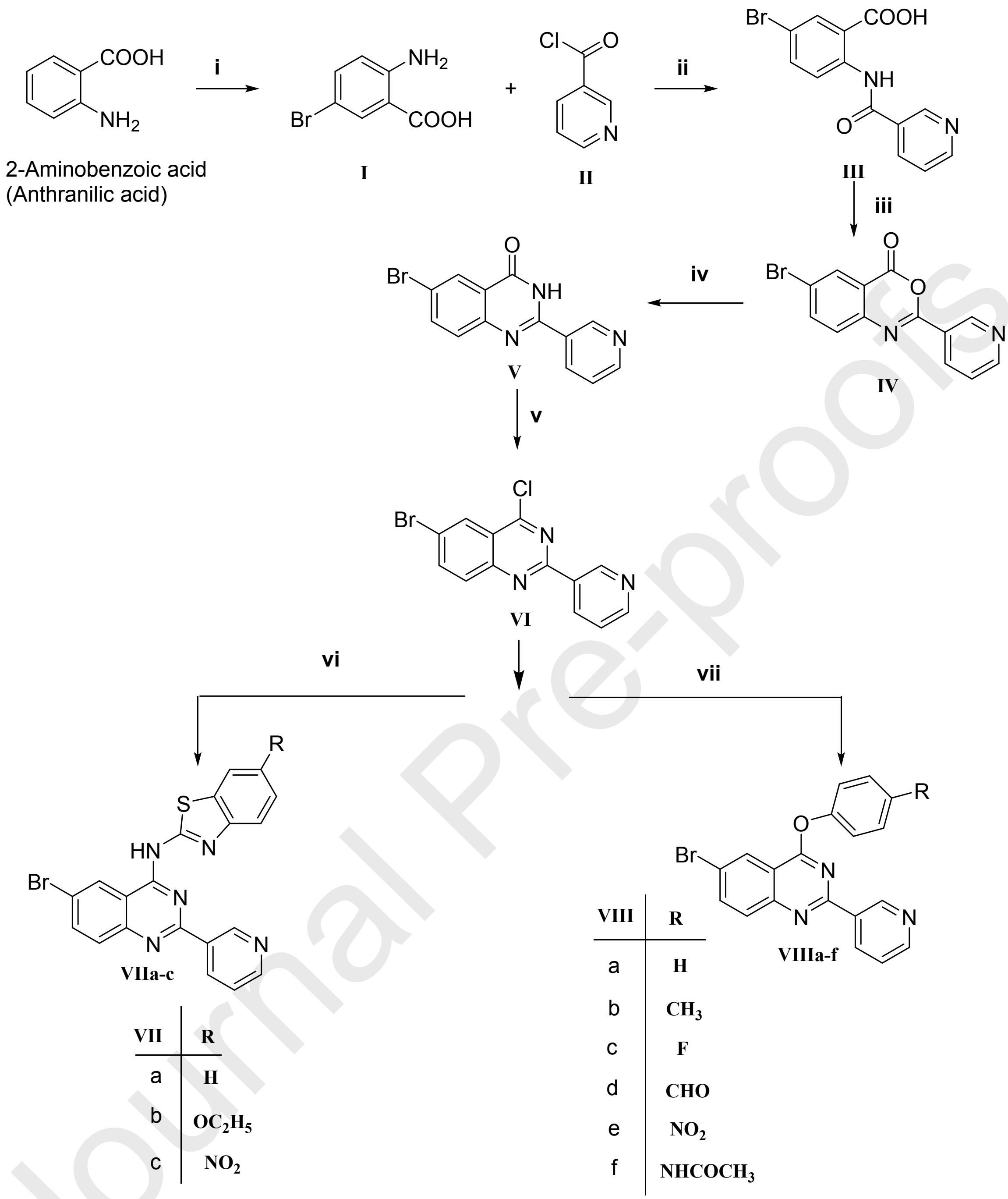

Scheme 1: Synthesis of the intermediates **I, II, III**, **IV**, **V, VI** and the target compounds **VIIa-c and VIIIa-f**; Reagents and conditions: (**i**) Br_2, glacial acetic acid, ice bath; (**ii**) Methylene chloride, triethylamine, 24 h RT; (**iii**) Acetic anhydride, reflux 4.5 h; (**iv**) Formamide, reflux 2.5 h; (**v**) $POCl_3$, reflux 2.5 h; (**vi**) appropriate 2-amino benzothiazole derivatives, DMF, anhyd. K_2CO_3, reflux 9 h; (**vii**) (un)substituted phenol derivatives, DMF, anhyd. K_2CO_3, stirr on cold 24 h.

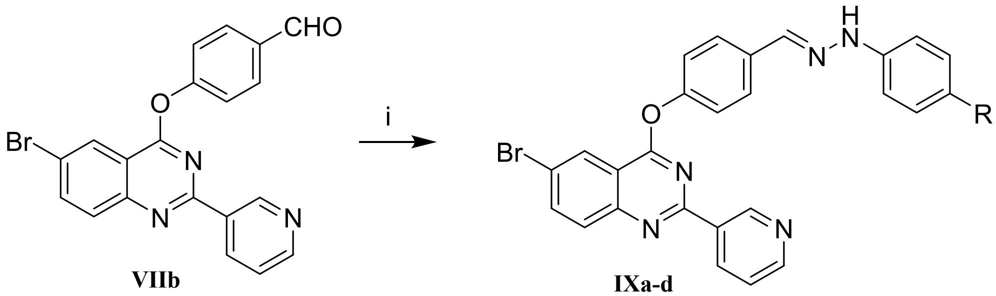

IX	R
a	H
b	Cl
c	OCH_3
d	SO_2NH_2

Scheme 2: Synthesis of the target compounds **IXa-d** from the target compound **VIIId**; Reagent and condition: (**i**) absolute ethanol, drops of glacial acetic acid, phenylhydrazine/4-hydrazinylbenzenesulfonamide, reflux 9.5-15 h. 4-chlorophenylhydrazine/4-methoxyphenylhydrazine, stirr on cold 24 h.

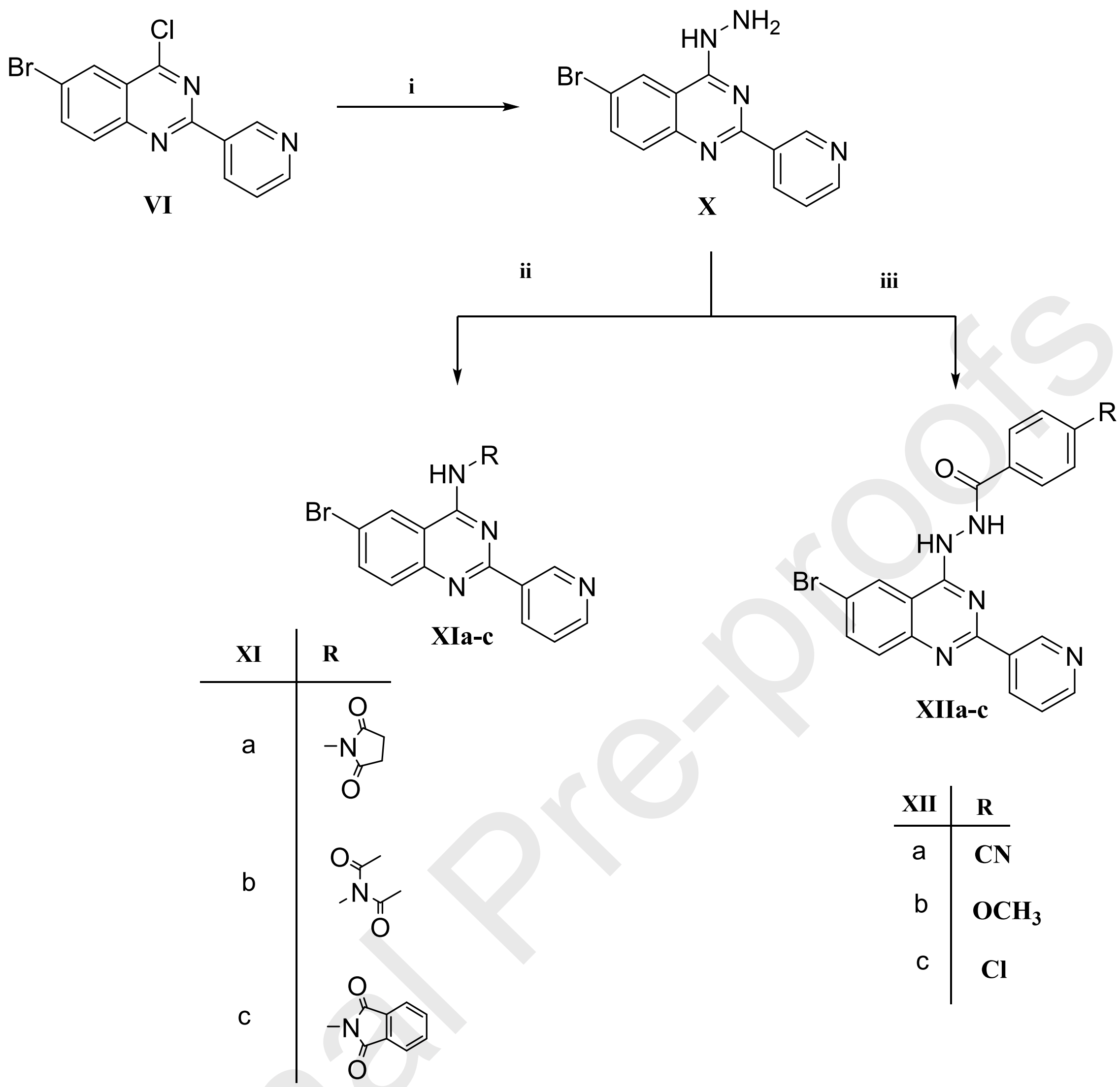

Scheme 3: Synthesis of the new intermediate compound **X**, the target compounds **XIa-c** and **XIIa-c**; Reagents and conditions: (**i**) NH_2NH_2 99%, reflux 8.5 h; (**ii**) acid anhydride, glacial acetic acid, reflux 4-13 h; (**iii**) appropriate 4-substitutedbenzoylchloride, methylene chloride, triethylamine, stirr on cold 10-72 h.

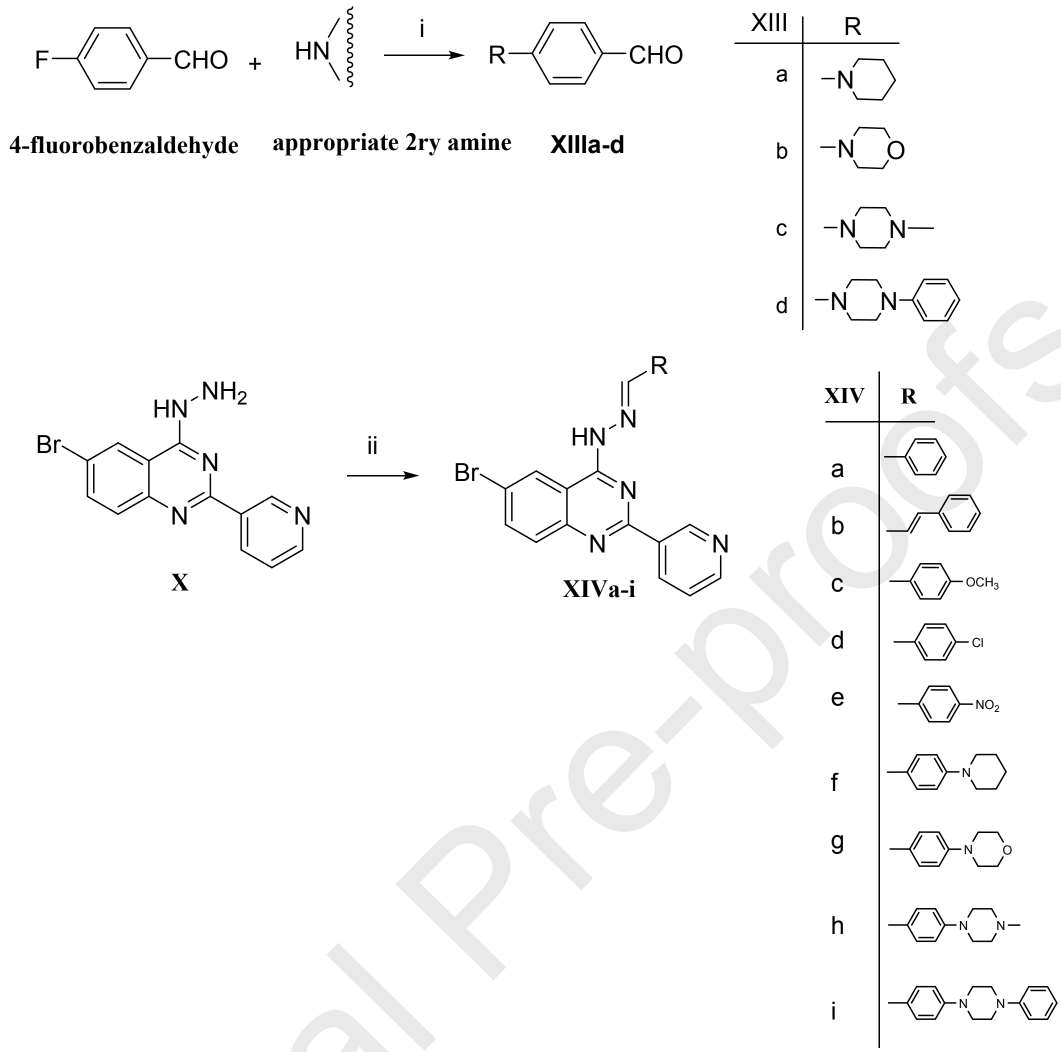

Scheme 4: Synthesis of reported aldehydic reagents **XIIIa-d** and the target compounds **XIVa-I**; Reagents and conditions: (**i**) DMF, anhyd. K_2CO_3, reflux 6-7 h; (**ii**) appropriate aldehyde, absolute ethanol, reflux 10-17 h.

Table 1: EGFR inhibitory activity of the target compounds compared to **Gefitinib** as a reference standard.

Cpd. No.	EGFR IC_{50} (µM)	Cpd. No.	EGFR IC_{50} (µM)	Cpd. No.	EGFR IC_{50} (µM)
VIIa	0.096 ± 0.00278	**IXb**	0.431±0.01241	**XIVb**	0.258 ± 0.00992
VIIb	0.454 ± 0.01309	**IXc**	0.303±0.00874	**XIVc**	0.573 ± 0.01651
VIIc	0.339 ± 0.01303	**IXd**	0.231±0.0087	**XIVd**	0.296 ± 0.01138
VIIIa	0.483 ± 0.01391	**XIa**	1.748 ± 0.06714	**XIVe**	0.141 ± 0.00408
VIIIb	0.818 ± 0.02356	**XIb**	0.461 ± 0.01771	**XIVf**	0.183 ± 0.00527
VIIIc	1.983 ± 0.07618	**XIc**	0.331 ± 0.01274	**XIVg**	0.289 ± 0.01111
VIIId	0.728 ± 0.0279	**XIIa**	0.303 ± 0.00874	**XIVh**	1.246 ± 0.04785
VIIIe	0.660 ± 0.01902	**XIIb**	0.292 ± 0.00843	**XIVi**	0.282 ± 0.00812
VIIIf	0.149 ± 0.00429	**XIIc**	0.286 ± 0.01099	**Gefitinib**	0.166 ± 0.00638
IXa	2.962 ± 0.11374	**XIVa**	0.796 ± 0.03058		

Table 2: Mutant EGFR inhibitory activity of the target compounds compared to **Gefitinib** as a reference standard.

Cpd. No.	IC_{50} (uM)	
	T790M	**L858R**
VIIa	0.02815±0.00069	0.055.14±0.00136
VIIIf	0.04768±0.00118	0.01172±0.00029
XIVe	0.02489±0.00061	0.04191±0.00103
Gefitinib	0.0232±0.00057	0.01819±0.00045

Table 3: Cytotoxicity of the tested compounds and **Gefitinib** against **A549, MCF-7, WI38, PC9** and **HCC827** cell lines and the selectivity index **(SI*)** for the tested compounds and **Gefitinib** relative to normal cell line**.**

SI* = activity of the tested compounds (IC_{50}) against normal cell line **(WI38)/**activity of the tested compounds (IC_{50}) against cancer cell line.

Cpd. No.	**IC_{50} (uM)**					**Selectivity index (SI)**	
	A549	**MCF-7**	**WI38**	**PC9**	**HCC827**	**A549**	**MCF-7**
VIIa	178.34 ± 8.9	2.49 ± 0.12	82.8 ± 4.14	1.05±0.02	3.43±0.066	0.464	33.253
VIIc	24.55 ± 1.22	3.195 ± 0.15	268.8 ± 11.6	NA	NA	10.949	84.131
VIIIf	29.16 ± 1.45	19.03 ± 0.95	57.72 ± 2.88	4.02±0.077	1.21±0.023	1.979	3.033
IXc	6.36 ± 0.21	1.89 ± 0.03	45.53 ± 1.28	NA	NA	7.158	24.089
IXd	5.774 ± 0.28	9.996 ± 0.44	56.80 ± 2.71	NA	NA	9.837	5.682
XIc	28.206 ± 1.41	10.142 ± 0.46	53.86 ± 2.6	NA	NA	1.909	5.310
XIIa	33.961 ± 1.69	6.881 ± 0.34	50.89 ± 2.21	NA	NA	1.498	7.395
XIIb	10.77 ± 0.52	8.22 ± 0.17	21.49 ± 0.92	NA	NA	1.995	2.614
XIIc	10.514 ± 0.52	2.517 ± 0.12	36.57 ± 1.61	NA	NA	3.478	14.529
XIVb	9.151 ± 0.45	11.879 ± 0.51	40.20 ± 1.84	NA	NA	4.393	3.384
XIVd	63.572 ± 3.17	0.956± 0.04	27.69 ± 1.33	NA	NA	0.435	28.964
XIVe	3.50 ± 0.17	20.48 ± 1.02	64.68 ± 3.23	3.66±0.071	5.49±0.11	18.480	3.158
XIVf	12.31 ± 0.61	56.50 ± 2.82	63.26 ± 3.16	NA	NA	5.139	1.119
XIVg	5.585 ± 0.27	45.559 ± 2.14	70.32 ± 3.34	NA	NA	12.590	1.543
XIVi	2.47 ± 0.06	8.42 ± 0.24	20.92 ± 0.77	NA	NA	8.469	2.484

Gefitinib	4.389 ± 0.21	4.972 ± 0.24	34.95 ± 1.72	1.36±0.02	3.99±0.07	7.963	7.029

Table 4: Cell cycle analysis results of compound **VIIa** after 24 h in **MCF-7** cell line.

Cpd. No.	%G0-G1	%S	%G2/M	%Pre-G1	Comment
VIIa	27.29	31.25	41.45	24.19	Pre G1 apoptosis and Cell growth arrest at G2/M.
Control	53.89	39.01	7.1	1.47	

Table 5: Effect of compound **VIIa** on apoptotic induction compared to the control cells after 24 h.

Cpd. No.	Apoptosis			Necrosis
	Total	Early	Late	
VIIa / MCF7	24.19 %	6.27 %	15.64 %	2.28 %
Control /MCF7	1.47 %	0.87 %	0.26 %	0.34 %

Table 6: Docking energy scores (*S*) in kcal/mol, interacting amino acid, Distances in Å, H-bond energies in kcal/mol of the tested compounds, **Gefitinib** and **Lapatinib** and their EGFR inhibitory activity (IC_{50} µM).

Compound	Docking score (*S*) (kcal/mol)	Interacting amino acids	Distances (Å)	H-bond energies (kcal/mol)	EGFR IC_{50} (µM)
VIIa	−12.74	Asp855 Met793	3.28 2.99	−1.6 −4.3	0.096
VIIc	−12.34	Asp855 H_2O Met793	2.80 3.13 3.22	−5.7 −1.4 −3.7	0.339
VIIIf	−11.49	H_2O Met793	3.18 3.41	−1.2 −2.3	0.149
IXb	−10.49	Met793	2.80	−3.8	0.431
XIc	−13.00	Asp855 H_2O Met793	2.70 3.14 3.31	−6.4 −1.4 −3.1	0.331
XIIb	−12.44	Asp855 H_2O Met793	2.73 3.12 3.22	−6.2 −1.5 −3.8	0.292
XIVe	−12.38	Asp855 H_2O Met793	2.78 3.14 3.34	−5.9 −1.4 −2.9	0.141
Gefitinib	−12.89	H_2O Met793	2.93 3.29	−1.1 −3.6	0.166
Lapatinib	−15.12	H_2O Met793	2.79 2.96	−1.4 −5.4	NA*

NA* = Not available.

Conflict of Interest

The authors have declared no conflict of interest

Corresponding author

Heba Abdelrasheed Allam

Department of Pharmaceutical Chemistry

Faculty of Pharmacy, *Faculty of Pharmacy, , Kasr El-Aini Street,*

Cairo University,

Cairo, 11562, Egypt

Tel. +201006377655

E-mail: hebaallam80@hotmail.com

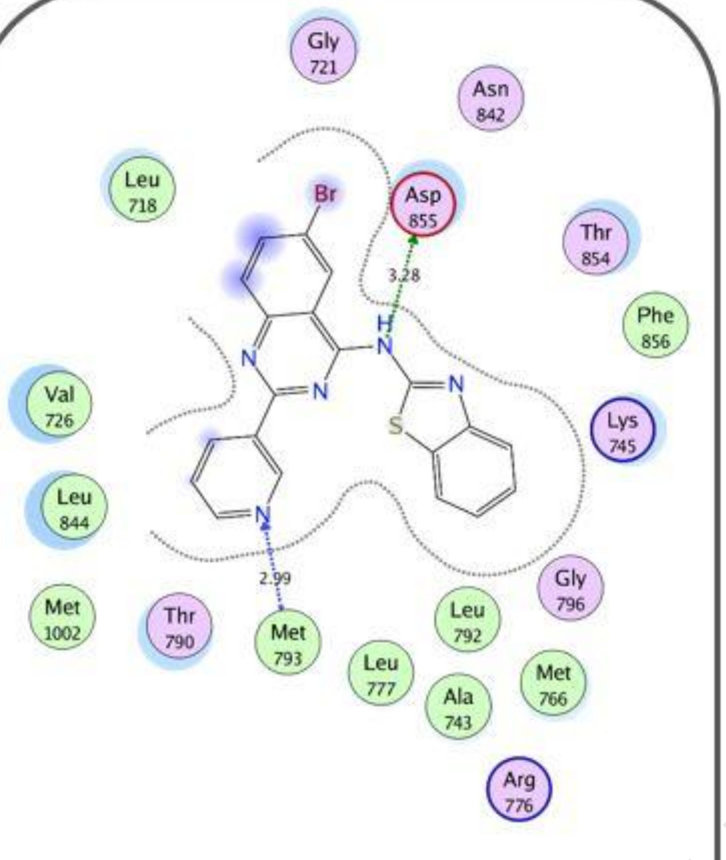

2D diagram of compound VIIa in the EGFR binding site

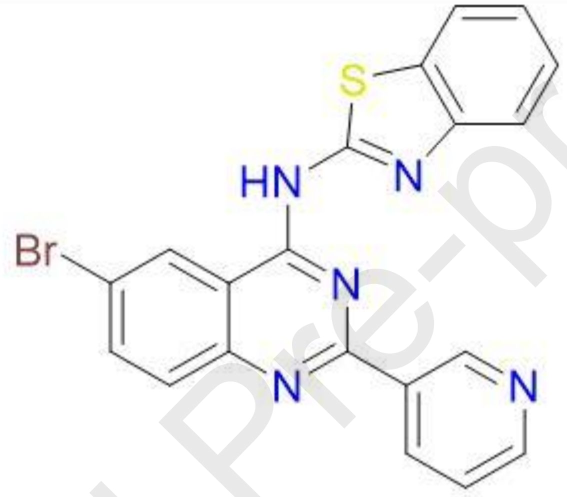

VIIa

EGFR IC_{50} 0.096 ± 0.00278 μM
MCF-7 IC_{50} 2.49 ± 0.12 μM
Selectivity index (SI) 33.253

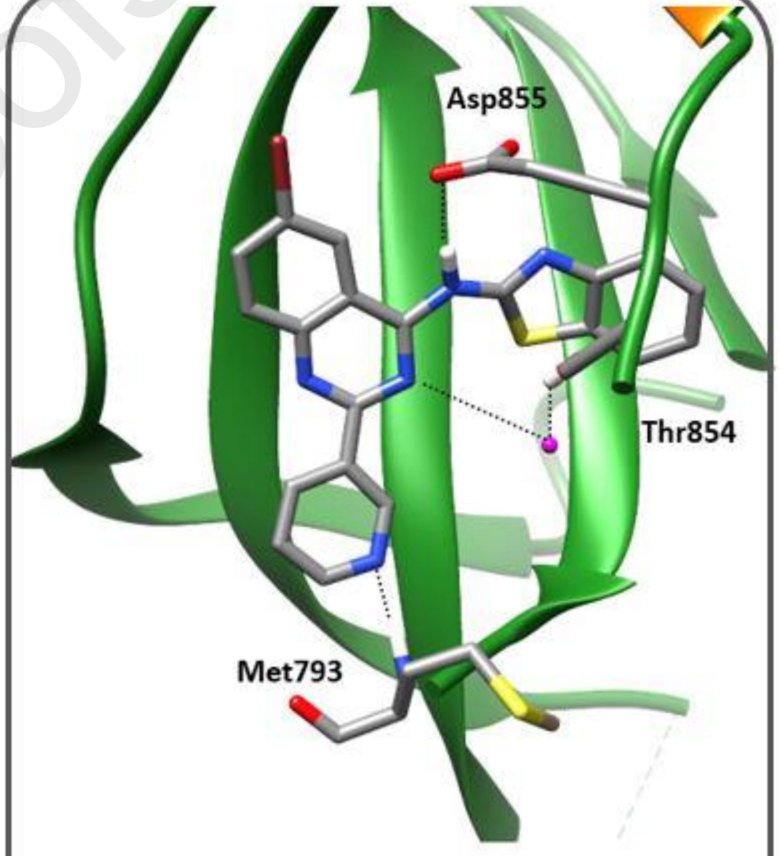

3D representation of compound VIIa in the EGFR binding site